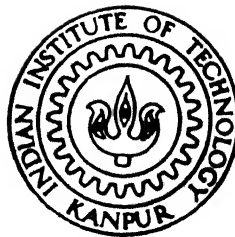


SPHEROIDAL WEATHERING OF DECCAN BASALT IN SAGAR AREA, M. P.

by

ASIM CHATTERJEE



DEPARTMENT OF CIVIL ENGINEERING

INDIAN INSTITUTE OF TECHNOLOGY KANPUR

DECEMBER, 1996

TH
CE/1996/m.
C.3325
1996
M
CHA
SPH

SPHEROIDAL WEATHERING OF DECCAN BASALT IN SAGAR AREA, M. P.

*A thesis submitted
in partial fulfillment of the requirements
for the degree of*

MASTER of TECHNOLOGY

by

ASIM CHATTERJEE

to the
**DEPARTMENT OF CIVIL ENGINEERING
INDIAN INSTITUTE OF TECHNOLOGY, KANPUR**
December, 1996

21 JAN 1967
CENTRAL LIBRARY
U. S. AIR FORCE
ICE No. 122866

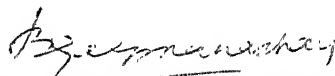


A122866

CE-1596-M-CHA-SPH

CERTIFICATE

Certified that the work presented in this thesis entitled **“SPHEROIDAL WEATHERING OF DECCAN BASALT IN SAGAR AREA, M.P.”** has been carried out by **Sri Asim Chatterjee** (Roll. No. 9510306) under my supervision and it has not been submitted elsewhere for a degree.




Dr. Bikash C. Raymahashay

Professor

Department of Civil Engineering

Indian Institute of Technology,

Kanpur - 208016

13.12.96


ACKNOWLEDGEMENT

It gives me immense pleasure to express my heartiest gratitude to Prof. B.C. Raymahashay for his valuable guidance and encouragement throughout the course of this work. His clear deep insight into many problems encountered during the period of work enabled me to accomplish this thesis work successfully.

My field trip was made possible because of valuable information and suggestion provided by Prof. S.K. Lunkad, Department of Geology, Kurukshetra University. I express my special thanks to him. I am thankful to Prof. P.O. Alexander and Dr. Prabhat Diwan, Department of Applied Geology, Sagar University, for providing me necessary field guidance, literature and toposheets.

I also wish to thank Dr. V.S.R. Murthy, Department of Materials and Metallurgical Engineering, IIT Kanpur, for initiating ideas, several discussions and suggestions at different stages of my work. I wish to express my profound gratitude to Dr. R.P. Singh and Dr. Rajiv Sinha of Civil Engineering Department for providing timely help and facilities. The reprints sent by Prof. S. S. Augustithis of Theophrastus Publications, Athens, Greece were of great help for my thesis work.

I am extremely grateful to Mr. Umashankar of X-ray laboratory, Mr. P.K. Paul of SEM laboratory and Mr. R.P. Singh of EPMA laboratory of Advanced Centre for Materials Science, IIT Kanpur. Mr. S.D. Dubey and late Mr. M.L. Srivastava from Engineering Geology laboratory deserve words of appreciation for their invaluable contribution in my laboratory work. I also acknowledge Mr. Verma of Civil Engineering Department for doing the drafting work. I am also indebted to the Department of Earth Sciences, University of Roorkee, for providing laboratory facilities.

Lastly, I would like to thank Saroj, Pradeep, Vikrant Jain, Umesh Singh, Prathiba, Mandal, Mishraji, Atanuda, Sahooji, K.K. Bhaia and all those who directly or indirectly helped in successful completion of my thesis work.

DECEMBER, 1996
IIT, KANPUR


ASIM CHATTERJEE

CONTENTS

LIST OF FIGURES

LIST OF TABLES

LIST OF PLATES

ABSTRACT

CHAPTER	PAGE No.
1 INTRODUCTION	
1.1 DECCAN BASALT	1
1.2 SPHEROIDAL WEATHERING	2
1.3 OBJECTIVES OF THIS STUDY	3
2 LITERATURE REVIEW	
2.1 DECCAN VOLCANISM	4
2.1.1 Geological setting	4
2.1.2 Petrography	6
2.1.3 Secondary Minerals	7
2.1.4 Chemical Characters	7
2.2 COOLING AND COLUMNAR JOINTING IN BASALT	8
2.3 WEATHERING, SOIL FORMATION AND WATER QUALITY	12
2.4 EXFOLIATION AND SPHEROIDAL WEATHERING	14
2.5 WEATHERING RIND	15
2.6 GEOLOGY OF THE STUDY AREA	18
2.6.1 Regional Geology	18
2.6.2 Topography	20
2.6.3 Drainage	23
3 METHODOLOGY	
3.1 FIELD WORK	25
3.1.1 Location, Climate and Local Geology	25
3.1.2 Sample Collection	28
3.2 LABORATORY WORK	28
3.2.1 Study of Rock Samples	29
3.2.2 Study of Soil Samples	30
3.3 COMPUTER BASED MODEL	31
4 RESULTS AND DISCUSSION	
4.1 DESCRIPTION OF THE FLOWS	32
4.1.1 6th Flow	32

4.1.2 7th Flow	33
4.1.3 8th Flow	34
4.1.4 9th Flow	34
4.2 MINERALOGICAL AND TEXTURAL STUDIES	34
4.2.1 Fresh Rock Core	36
4.2.2 Intermediate Weathering Product	38
4.2.3 Final Weathering Product	41
4.3 GEOCHEMICAL CHANGES ACROSS THE CORE-RIM INTERFACE	46
4.4 VOLUME CHANGE DURING WEATHERING REACTIONS	49
4.5 THREE MINERAL COMPUTER MODEL	53
5 SUMMARY AND CONCLUSIONS	
5.1 MINERALOGY, TEXTURE AND GEOCHEMICAL CHANGE	55
5.2 OVERALL MECHANISM OF SPHEROIDAL WEATHERING	58
5.3 SUGGESTION FOR FURTHER WORK	58
REFERENCES	60
APPENDIX - I	
APPENDIX - II	

LIST OF FIGURES

Figures	Page No.
Fig. 2.1 Location map of Deccan Basalt showing study area	5
Fig. 2.2 Development of spherical boulders by weathering of rock cubes	16
Fig. 2.3 Stages in the formation of a conical hill in the Deccan trap by scarp retreat	21
Fig. 3.1 Geological map around Sagar University campus showing location of sampling sites	26
Fig. 4.1 XRD pattern of fresh rock core	37
Fig. 4.2 XRD pattern of innermost rindlets	42
Fig. 4.3 XRD pattern of outer rindlets	42
Fig. 4.4 XRD pattern of red soil showing halloysite peaks	44
Fig. 4.5 XRD pattern of black soil showing glycol expansive beidellite peaks	45
Fig. 4.6 SEM-EDX across core-rim interface	48 b
Fig. 4.7 Schematic flow diagram of computer model	54

LIST OF TABLES

Tables	Page No.
Table 2.1 Stratigraphic succession of Sagar area	20
Table 4.1 Identification of X-ray peaks for fresh rock core	37
Table 4.2 Identification of X-ray peaks for partly weathered innermost rindlet	40
Table 4.3 Identification of X-ray peaks for partly weathered outermost rindlet	43
Table 4.4 Identification of X-ray peaks for red soil	44
Table 4.5 Identification of X-ray peaks for black soil	45
Table 4.6 Gist of mineralogy of the samples collected from different locations	46
Table 4.7 Chemical analysis of spheroidally weathered basalt, Phutkapahar, Central India	47
Table 4.8 List of $\Delta V\%$ values for different reactions	52
Table 4.9 Computer output	

LIST OF PLATES

Plates	Page No.
Plate 4.1 Spheroidally weathered boulders (7th flow)	33
Plate 4.2 Weathering profile (8th flow) showing reddish brown top soil	35
Plate 4.3 Spheroidal weathering profile (9th flow)	35
Plate 4.4 Cross section of spheroidally weathered boulders	38
Plate 4.5 Plagioclase alteration to clay minerals	39
Plate 4.6 Interface of fresh rock core and partially altered innermost rindlet	40
Plate 4.7 Scanning electron micrograph of halloysite	43
Plate 4.8a EPMA X-ray mapping showing elemental variation across core-rim interface	48 a

ABSTRACT

Four successive basalt flows occur in the Sagar area of Madhya Pradesh. They belong to the well known Deccan Basalt Province. Each flow shows typical exfoliation and spheroidal weathering features. This thesis work concentrated on the formation of spheroidal boulders by weathering of basalt.

Field observations followed by detailed laboratory study of the samples of the weathered rock and soil showed that spheroidal weathering is initiated by a process of mechanical weathering of jointed basalt but subsequent chemical weathering results in onion-skin shells around a core of fresh rock. Weathered products containing an assemblage of beidellite (smectite), halloysite (kaolinite) and iron oxide (goethite?) occupy a volume greater than the primary assemblage of Ca-plagioclase, augite and magnetite. This causes an internal stress within the rock mass which is essential for development of the thin shells which finally fall off.

The presence of primary and secondary minerals was established by hand specimen study, petrography, X-ray diffraction (XRD) and energy dispersive X-ray analysis under scanning electron microscope (SEM-EDX). Difference in elemental concentration along core-rindlet interface was investigated by X-ray mapping with electron probe micro analyser (EPMA). Based on these results, a computer-aided three-mineral model was developed which shows that a maximum volume expansion of 5.564% can be obtained when (i) the initial modal volume percentage of bytownite, augite and magnetite are 39.04, 45.87 and 14.74 respectively in the fresh rock, (ii) fraction of bytownite altered is 0.6, augite altered is 0.8 and magnetite altered is 1.0, and (iii) proportion of reactions of bytownite weathering to form beidellite is 0.50, augite weathering to form beidellite and goethite is 0.75 and magnetite weathering to form goethite is 1.00. During these reactions the initial modal volume percentage of plagioclase, augite and magnetite is responsible for the difference in weathering from flow to flow.

CHAPTER-1

INTRODUCTION AND OBJECTIVE

1.1 DECCAN BASALT:

The Deccan Basalt Province is a well known unit in Indian Geology. It is spread over vast areas in western, central and southern India. The total outcrop of around 512,000 sq. km. is mainly occupied by a volcanic igneous rock of basaltic composition. The rock is fine grained and dark coloured, composed essentially of calcic plagioclase, clinopyroxene and magnetite along with interstitial volcanic glass.

In addition to its importance in geology, Deccan basalt has drawn the attention of civil engineers because this rock forms the bedrock for major projects like dams, tunnels, railways etc. and it is used as road metals and construction materials including concrete aggregates. Among rocks, basalt is known to have one of the highest compressive strengths ($>2800 \text{ Kg/cm}^2$). On the other hand its main constituents like volcanic glass, plagioclase feldspar and pyroxene are highly weatherable under earth's surface condition. It is therefore very important to distinguish between fresh and weathered basalt for any scientific investigation.

In a broad sense a rock during weathering loses strength, becomes more deformable and permeable to ground water percolation. The ultimate product of chemical weathering of basaltic rocks is an expansive soil (Black Cotton Soil) containing swelling clays which has its own characteristic problems in engineering projects.

Much work has been done regarding petrology, mineralogy, major and trace element geochemistry, palaeomagnetism, gravity anomalies, engineering properties,

groundwater quality and soil formations within the Deccan Basalt Province. However, there is a knowledge gap on the initial stages of rock decomposition, which is characterised by typical '*spheroidal weathering*' of basalt outcrops.

1.2 SPHEROIDAL WEATHERING:

Spheroidal weathering starts along intersecting joint planes in basalt and proceeds after initially rounding off the edges and corners and then producing thin concentric shells or layers which crumble and fall off gradually resulting in an onion-skin morphology of altered layers enveloping a core of fresh rock. This phenomenon of weathering has a number of synonym in testimony to different appearance of weathered rock in outcrops such as “weathering rings”, “weathering crusts”, “diffusion rings” or “weathering rinds”. There is a general feeling that the exfoliation of the original rock leading to the development of concentric shells results from pressures set up within the rock during chemical weathering. The origin of these pressures may be related to the fact that the weathering products occupy a greater volume than that of the original rock (Leet & Judson, 1969; Skinner & Porter, 1995).

Keeping this state of knowledge in mind, an attempt has been made to carry out a detailed study of the mineralogy, texture and chemical changes within the microweathering environment of spheroidally weathered basalt in a typical outcrop. For this purpose, the Sagar area of Malwa plateau in Madhya Pradesh was selected for fieldwork, mainly because of the easy accessibility of road sections, quarry sites and availability of earlier data on petrology and related aspects. It is expected that the information collected during this work will clarify some of the mineralogical aspects including chemical weathering of

primary minerals which leads to the generation of stress due to expansion. This stress appears to be essential for spheroidal weathering at the incipient stages.

1.3 OBJECTIVES OF THIS STUDY:

The main objectives of this work can be listed as follows:

- To collect representative samples of spheroidally weathered boulders, intermediate weathering products as well as soils, which indicate the more advanced stage of weathering in a complete profile.
- To characterise chemical and mineralogical changes in weathered boulders by utilising standard techniques such as X- ray diffraction, microprobe analysis, optical and electron microscopy.
- To identify appropriate weathering reactions relating primary and secondary minerals which cause volume expansion within the microweathering environment.
- to quantify volume change in terms of a computer-aided model.
- To synthesise the results obtained in terms of an overall mechanism of spheroidal weathering at microlevel on basaltic country rocks.

CHAPTER-2

LITERATURE REVIEW

2.1 DECCAN VOLCANISM:

2.1.1 Geological setting:

The enormous lava flows of basaltic composition spreading over a vast area of the order of half a million (512, 000) sq. km. in the western, central and southern part of India are known as Deccan Basalt in Indian geology because of their geographic location (Fig.2.1). They issued through long narrow fissures or cracks resulting due to tension in earth's crust, and are therefore called "fissure eruptions". The lavas spread out far and wide as horizontal sheets. Because of their tendency to form flat topped plateau like features and their dominantly basaltic composition, the rocks are classified as "Plateau Basalt". The flows are called traps because of their 'step-like' or 'terraced' appearance of their outcrops, the term being of Scandinavian origin (Krishnan, 1982). Differential weathering and erosion have removed the basalt at places and exposed the underlying older rocks. Thus a number of detached outliers occur, which are separated from the main mass by wide distances. The present distribution of traps, therefore, is not true representative of their past extension which has been calculated to have been over 1.5 million sq. km. The lava was not erupted in a single phase because there are several distinct flows in a given section. The different flows are separated by ash beds/scoriae and lacustrine sediments called intertrappean beds.

It is believed that the eruption of Deccan Basalt was associated with the break up of the ancient southern continent of Gondwanaland about 60-100 Ma. ago. The eruption

was mainly of 'fissure type'. However, a few localized instances of 'central type' have been reported by some workers. Field criteria and petrographic evidences show that the lava flows might have been erupted subaerially.

Sukheswala (1981) concluded that the first magma to erupt on a wide scale was of tholeiite type (silica rich basalt). This was followed by rhyolite, and finally the igneous activity closed with minor quantities of the alkali olivine basalt magma and the carbonatite alkalic magma occurring as small plugs within the tholeiite. These four magma types came as independent entities without any known genetic link existing between them. Earlier studies have revealed that these Deccan lavas perhaps erupted mainly through three tectonic lineaments marked by i) the ENE-WSW trending Narmada-Son lineament-cum-graben belt, ii) the N-S trending Konkan and off-shore block faulted belt, iii) the NNE-SSW trending Cambay graben belt (Krishnaswamy, 1981). These three major tectonic belts show positive gravity anomalies and it is well established that there are deep rooted faults and shear zones. The traps have been classified by earlier workers as upper, middle and lower on considerations of stratigraphy and presence of intertrappeans. Paleomagnetic data and chemistry of basalt also helped to subdivide the traps.

2.1.2 Petrography:

The Deccan basalts are generally dark grey, dark greenish-grey, totally black, and less commonly brown to purplish in colour with an average specific gravity of 2.9. In parts of western India including Gujarat and Kutch, localized examples of associations of traps with more acid, intermediate, basic and ultrabasic differentiates have been reported. The non vesicular ones are comparatively softer and break more easily.

The basaltic rock typically has a porphyritic texture with phenocrysts of calcic plagioclase and less frequently of augite type pyroxene in a matrix containing fine grained plagioclase, augite and partly devitrified glass (Krishnan, 1982). Among opaque minerals granular, square and rod like small size crystals of ilmenite and magnetite are commonly disseminated throughout the groundmass. The glass occurs in the interstices of groundmass crystals. Its colour is varied-red, orange, yellow and brownish black - the last due to dusty opaques. The two minerals augite and magnetite are together represented in the glass (Krishnan, 1982). The rock is generally free from olivine, although, West, quoted by Krishnan (1982), has described local occurrences of basalt containing phenocrysts of plagioclase, pyroxene and olivine.

2.1.3 Secondary Minerals:

Secondary minerals occur either as infillings of the vesicles, usually towards the top of the individual flow, or as the products of alteration and replacement. Such zones of secondary minerals serve to differentiate and demarcate one flow from the other. The secondary minerals of hydrothermal origin are zeolite, calcite, chalcedony, opal, quartz and amethyst. The alteration products are chlorophaeite, palagonite, celadonite, iddingsite and serpentine. The last two are formed from olivine and the rest presumably from the glass. Yellowish brown, pale yellow and greyish green chlorophaeite at times are pseudomorph after pyroxene crystals (Durge, 1987).

2.1.4 Chemical Character:

The first systematic study of the petrochemical characters of Deccan traps was made by Washington in 1922, as mentioned by Najafi et. al. (1981). He studied 22

specimens of Deccan traps collected from different locations. He drew attention to the remarkable uniformity of their chemical characters and described them as tholeiitic basalt. Petrochemical studies made in 1947 by Vemban, quoted by Krishnan (1982), led him to conclude that the original magma was picritic in composition, and both the lines of differentiation i.e calc-alkali and alkali-olivine trend were present. On the basis of high quality analysis of 73 samples of the basalt in Bombay region by Sukheswala and Poldervaart in 1958, as quoted by Alexander (1977), it was concluded that lavas of intermediate compositions are rare in Deccan province and that iron enrichment is generally more pronounced than alkali enrichment. Subsequently several analyses of Deccan basalt clearly indicated that the Deccan traps are not chemically uniform and it is not correct to group the entire Deccan traps under tholeiites. Obviously there are areas that form subprovinces in the main Deccan Basalt Province.

In 1964, Sinha and Karkare, quoted by Alexander (1977), furnished the first systematic account of the behaviour of the major and trace elements in the lower, middle and upper traps. Their study reveals that inspite of similarity in the mineral composition, there are diagnostic chemical variations both laterally and vertically. Alexander (1977) described the detailed geochemistry of ten lava flows around Sagar. Rare earth elements geochemistry has been dealt with by Alexander and Gibson in 1977 and Alexander in 1979 as quoted by Durge (1987).

2.2 COOLING AND COLUMNAR JOINTING IN BASALT:

The initial temperature of basaltic magma may be expected to be in the range of 1050°C to 1200°C as stated by Lovering (1955), quoted by Hess and Poldervaart (1967).

Recent measurements on Hawaiian lava gives the same range. As the basalt flow cools, it changes from a viscous liquid into a semibrittle solid. The solidification temperature of basalt is about 1000°C . If the flow cools steadily and uniformly, the solidifying layers develop a uniform tension. The tensile strength of basalt ($60\text{-}300\text{Kg}/\text{cm}^2$) is much less than its compressive strength ($800\text{-}3000\text{Kg}/\text{cm}^2$) (Jumikis, 1979) When this level is exceeded, a network of cracks forms. The orientation of the most numerous joints/cracks is normal to the cooling surfaces of the flow. This suggests that they are primarily due to shrinkage on cooling. Billings (1990) described that a similar process must have accounted for the development of mudcracks, which form during the desiccation and associated contraction of the surface layers of mud.

The spacing of the joints depends to some extent on the thickness of the flow. The joints develop progressively as the flow cools and the number and width of the joint gradually increases. Secondary joints commonly develop from the primary ones, breaking the mosaic into smaller and smaller blocks.

Tension joints are very common in Deccan lava flows, which split the rock into long prisms or columns termed as 'columnar joints'. Some more details of columnar jointing are discussed in the following paragraphs.

Columnar joints form remarkable polygonal pattern that vary from being tetragonal to nearly hexagonal. However, the hexagonal form of columnar jointing is most common. In many parts of the world, thick basalt lava flows having well developed columnar jointing have long impressed scientists and laymen. Classical examples are the Giant's Causeway in Northern Ireland; Fingal's Cave on the Island of Staffa; the Devils Postpile in

the Sierra Nevada of California; flows of Columbia River region and flows of Bombay and Malwa region of India. Some of these sites have recently been designated as national parks. In addition to the aesthetic qualities of the columnar joints, a detailed understanding of the mechanism of columnar joint formation has important geologic and engineering application.

Columnar jointing is rare in thin lava flows, but it is common in thin dikes and sills. Perfection of columnar jointing is related to the rate of cooling although that is probably not the only factor involved. There are some examples of good columnar structure that are in somewhat thinner flows that filled the valleys as that apparently poured into the ocean. Evidences from some regions suggests that good columnar jointing was formed only where the underlying surface was saturated with water. The more effective cooling brought about by water seems to have been the factor that, in the marginal cases, determined joint formation.

Columnar jointed flows generally show a two-tired or three tired arrangement. Tomkeiff (1940), quoted by Hess and Poldervaart (1967) gave different names to them. At the bottom, a set of thick and usually well formed columns stands essentially normal to the base of the flow and is known as “colonade”. Above it is a layer of thinner and less regular columns that may be essentially normal to the flow top but may show much irregularity of arrangement is known as “entablature”. Commonly, the top of the flow shows jointing normal to the flow surface that is a coarse, or even coarser than that of the lower portion. The joints, in this uppermost portion may be columnar, or they may be irregular, like those in thin lava flows.

Beard (1959), quoted by Hess and Poldervaart (1967), stated that columnar joints most frequently have a hexagonal cross-section, with angles approaching 120° . But five sided, seven sided, eight sided and three sided columns are also occasionally found. The ideal geometry of hexagonal shape is still not well understood. As quoted by Smalley (1966), Holmes in 1965, described the formation of an ideal hexagonal pattern of joints by uniform contraction of lavas on cooling. The isotherms move gradually inward from the cooling surfaces and in igneous rocks the tensile stresses become oriented parallel to these isothermal surfaces during cooling. Rapid cooling, occurring within thin flows and at the surface of thick ones, producing irregular or at most very crudely columnar jointing. Slower cooling results in a gradual accumulation of tension and when tension reaches a certain critical level (depending on temperature, degree of crystallinity of the flow and probably other factors), rupture occurs.

As stated by Theiss and Moores (1992), igneous rocks generally tend to form tensile fractures perpendicular to the surface of equal temperatures, as the rocks are weaker in tension than in compression. The close packed fracture bounded hexagonal prism has the smallest fracture surface area per unit volume of the prism shapes (see appendix I). Thus, hexagonal network of cracking gives maximum energy release, and this form of columnar joint is dominant. Unlike ideal cases, the temperature of lava flows are not uniform in nature. So, cracking initiates in some parts before others. Set of cracks forming independently of one another are unlikely to meet to form an ideal hexagonal network.

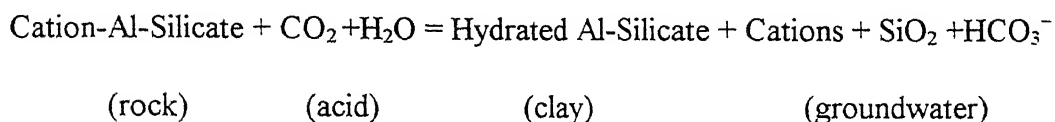
2.3 WEATHERING, SOIL FORMATION AND WATER QUALITY:

According to Krauskopf (1982) weathering is defined as the reaction of rocks and minerals with the constituents of air and water at or near the earth's surface. This means the approach of equilibrium in a system involving rocks, air and water. There are two general types of weathering: physical and chemical. It is hard to separate these two types in nature, for they often go hand in hand, though in some environments one or the other predominates.

Physical or mechanical weathering, which is also referred to as disintegration, is the process by which a rock is broken down into smaller and smaller fragments as the result of energy developed by physical forces. Physical weathering of rock is common in nature and is accomplished by alternate freeze and thaw, heating and cooling, mechanical action of organisms and impact of rain drops, lightning etc.. On the other hand, chemical weathering, sometimes called decomposition, is more complex. Chemical weathering actually transform the original material into something different and some of the constituents are dissolved and carried away in solution, thus influencing water quality. The major processes involved are carbonation, oxidation and hydration.

In basaltic rock, which has a relatively high temperature of crystallization, the constituent minerals like olivine, pyroxene and Ca-rich plagioclase are most unstable. They are, therefore most weatherable as listed in the Goldich Weatherability Series discussed by Krauskopf (1982).

Among various agents of chemical weathering, CO₂ saturated water occurring as rain or groundwater is most effective. The CO₂ is derived from atmosphere as well as from the decay of organic matter in soil zone. Dissolution of CO₂ gas in water produces the weak acid H₂CO₃ which undergoes dissociation in two steps. This dissociation supplies H⁺ ions which are responsible for the breakdown of rock forming minerals (Raymahashay, 1996). Following the pioneering work of Garrels and Christ (1965), chemical weathering of silicate minerals is usually represented as an acid attack:



The net result of chemical weathering is thus an assemblage of clay minerals in soils and accumulation of dissolved ions in groundwater.

It has been observed that two types of residual soils develop by weathering of Deccan basalt. Under poor drainage conditions at the foot hills, the accumulated cations tend to form the complicated structure of smectite clays. They constitute expansive soils commonly known as 'Black Cotton Soil'. On the other hand, well drained slopes and hill tops are covered with a red coloured 'Lateritic Soil' rich in kaolinite group of clays and Al/Fe oxides. The relationship between thermodynamic stability of clay minerals and groundwater quality in weathered Deccan basalt of Malwa plateau has been discussed by Lunkad and Raymahasay (1978).

Later work by Shukla (1993) concentrated on the characteristic of Red Bole horizons sandwiched in between successive Deccan basalt flows in the Pune region of Maharashtra. Sharp X-ray peaks of quartz and zeolite in these layers distinguish them

from a dark top soil developed over the upper basalt. Wilkins et. al. (1994), studied the detailed geochemistry of weathering regimes in the Deccan basalt and compared red bole horizons with laterites. They concluded that laterites represent an advanced stage of weathering, whereas, red boles are much less weathered. Pawar (1993), discussed the mechanism of carbonate precipitation in basaltic aquifer due to weathering of plagioclase, augite and zeolite.

2.4 EXFOLIATION AND SPHEROIDAL WEATHERING:

During weathering, concentric shells may spall off from the outside of an outcrop or a boulder, a process known as exfoliation. This produces large dome like hills, called exfoliation domes and rounded boulder at a smaller scale, usually referred to, as spheroidally weathered boulders. It seems that the forces that produce these two forms originate in different ways (Leet and Judson, 1969).

Joints in many massive rocks are broadly curved and run more or less parallel to the rock surface. As erosion strips away the surface cover, the downward pressure on the underlying rock is reduced. Thus, as the rock mass begins to expand, lines of fracture develops, marking off the slabs that later fall away. Finally a broad curved hill of bedrock develop.

In the case of spheroidal weathering, the boulders are rounded by the spalling off of a series of concentric shells of rocks. Here the shells develop as a result of pressure set up within the rock by chemical weathering; rather than by lessening of pressure from the above by erosion. When certain minerals are chemically weathered, the resulting product occupy a greater volume than the original material. So, this increase in volume creates the

pressure responsible for spheroidal weathering (Leet and Judson, 1965; Skinner and Porter, 1995). Since chemical weathering is maximum in the portions of the rock most exposed to the air and moisture, it is there that expansion and hence the number of shells are greatest.

Weathering generally starts with a cube of fresh rock, as water moves along joints and attacks the rock from all sides. The volume of unaltered rock will slowly decrease and the shape becomes more spherical as explained in Fig. 2.2. The results are often seen in fresh road cuts where rounded boulders produced by such progressive decomposition are often found in rows running in several directions. The pattern results from intersecting joint sets that control the slow movement of water through the rock. The size of the boulders is also controlled by the spacing of the joints.

Skinner and Porter (1995), discussed two important relationships (i) subdivision of large blocks increases the surface area and (ii) effectiveness of chemical weathering increases as the surface area exposed to weathering increases.

2.5 WEATHERING RIND:

Weathering rinds form a sequence of altered rocks physically attached to and encircling an inner core of comparatively fresh rock. Weathering begins at the freshly exposed surface of an unaltered boulder and proceeds slowly inward. Weathering rinds generally represent the first stages of chemical weathering and the early history of alteration of the fresh rock core are preserved in the weathering rind system (Fritz, 1985). This weathering commonly involves oxidation of iron rich minerals to produce goethite, which imparts a light brownish colour to the developing rind. Such a rind forms on all but

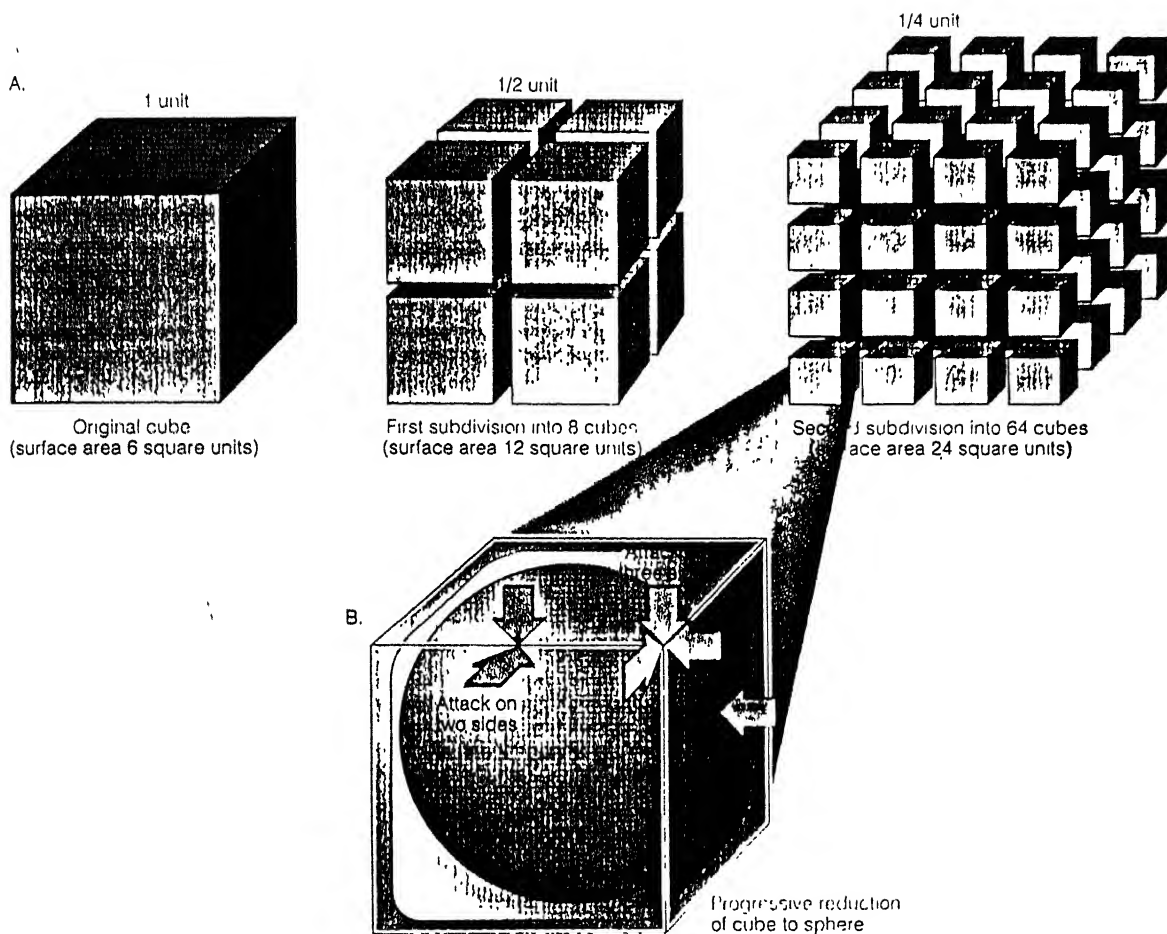


Fig. 2.2 Subdivision and weathering of rock cubes. A. Each time a cube is subdivided by slicing it through the centre of each of its edges, the aggregate surface area doubles. This greatly increases the speed of chemical reactions. B. Solutions moving along joints separating nearly cubic blocks of rock attack corners, edges and sides at rates that decline in that order, because the numbers of corresponding surfaces under attack are 3, 2 and 1. Corners become rounded, and eventually the blocks are reduced to spheres. Once a spherical form is achieved, the energy of attack becomes uniformly distributed over the whole surface, so that no further change in form occurs.

(Source: Skinner and Porter, 1995)

the most chemically stable rock types when chemical weathering attacks them. An exception is carbonate rocks, which dissolve under chemical attack, thereby preventing the formation of an obvious rind. In some rock types, the altered mineral matter in a developing rind crumbles away as the rock slowly weathers. In others, like fine grained basalt, the rind tends to remain coherent and becomes thicker as the weathering proceeds inward, attacking the solid unaltered core.

Augustithis and Ottemann (1966), were one of the first to study the diffusion rings in spheroidal weathering. They compared the mineralogical and X-ray fluorescence spectra between different weathering zones and suggested elemental migration as a possible cause of these ring formations. This was followed by the work of Augustithis and Vgenopouls (1983), who studied the leaching and diffusion-rings in different rocks.

Fritz and Ragland (1980), evaluated the relative importance of rock texture and mineralogy in influencing weathering rinds developed on plutonic igneous rocks. Besides, these, topography and climate may also influence the development of weathering rind on igneous rocks. They also described the orientation and propagation of solution channels in weathered rock which control the appearance of weathering rind development on that rock. Fritz and Mohr (1984) studied the chemical and mineralogical changes of innermost rindlets and the details of incipient alteration of minerals along solution channels of a spheroidally weathered anorthosite boulder from the Wichita Mountain, Oklahoma. Fritz (1985) studied the weathering rind characteristics of two mineralogically similar rock, adamellite and syenite in the North Carolina piedmont to determine the factors controlling their dissimilar types of alteration.

2.6 GEOLOGY OF THE STUDY AREA:

2.6.1 Regional Geology:

Deccan outcrop of Sagar area constitute the eastern fringe of Deccan trap. The regional geology of Sagar district has been described by Rajrajan, quoted by Durge (1987). Major parts of this district is occupied by two important supergroups. They are Vindhya and Deccan traps with intercalated intertrappean sediments. Occasionally, infratrappean Lameta group of rocks are also seen. Lateritic soil and alluvium constitute the uppermost and youngest formations in this district.

Vindhya occur in the form of exhumed ridges which were once covered by trappean lavas, since eroded. They are represented in this district by predominantly Rewa group of rocks namely, orthoquartzites and subordinately by shales. They are unfossiliferous and undisturbed and almost horizontal, with local dips upto 2°-5° being not uncommon. Sedimentary structures of shallow water origin such as ripple marks and current bedding are abundantly found in them. Orthoquartzite is very hard because its detrital quartz grains are cemented by silica cement. It is used both as road ballast and roofing material. Nine basaltic lava flows comprise the Deccan traps of Sagar district, having a total thickness of about 150-200 mts.. They constitute the typical flat topped, stepped slope hilly topography. Lava flows are generally horizontal and of variable thickness.

Intertrappeans indicate geological periods of no volcanic activity when temporary basins of sedimentation were established in the trappean ground surface of this district and

the sediments of variable thickness were deposited (few cms. to few ft.). The intertrappeans here comprise mostly of cherty limestone and minor clay and chert. Individual intertrappeans show variation in lithology laterally and vertically. Some fossils are also reported from them.

Intertrappean lameta beds are fluvatile or estuarine beds occurring below the traps. These are mainly impure limestones with subordinate clays. Limestones are arenaceous but at a few places, the pure variety is also found. Their thickness varies from place to place depending upon the original Vindhyan topography. Rarely they contain good determinable fossils, although Mollusca, Fishes and Dinosaurian reptiles have been found in the type area of Lametas from Jabalpur (Krishnan, 1982).

Lateritic soil constitutes the top of many flows as disconnected patches. A uniform thickness is not usual; it occurs as huge rounded boulders of ferruginous reddish brown colour with typical pisolitic structure. It is interesting to note that only 100 km. east of Sagar there are extensive economic deposits of bauxite derived from Deccan traps, but for some unknown reason, aluminous laterites are completely missing from around Sagar.

Alluvium, the youngest formation in this district is extensive, ranging in thickness from a few metres to 10 metres. The hill tops and plateaus are normally covered with lateritic soils. The traps at lower elevations are generally covered by thick clayey loam - the Black Cotton Soil or 'Regur', rich in plant nutrients such as lime, magnesia, iron and alkali. This is dark grey to black in colour, very sticky when wet and cracks easily on drying.

Table 2.1 gives the geological formations in the order of superposition in Sagar district.

TABLE 2.1 Stratigraphic Succession of Sagar Area

	Alluvium
Pleistocene and Recent	//////////Unconformity//////////
	Laterite
Upper Cretaceous	Deccan trap lava flows with intertrappean beds of limestone and clay
	//////////Unconformity//////////
Precambrian	Vindhyan sandstone - quartzite

After Durge, 1987

2.6.2 Topography:

As described by Subramanyan (1981), the landscape of Deccan trap country are characterised by conical hills, flat topped hills, plane areas and stepped topography. In the north eastern part the maximum elevation is 1124 m. near Amarkantak and minimum elevation is less than 300 m. along the Narmada valley around Hosangabad. Thus the relief is over 800 m.. There are many flows of basalt in this part with an average thickness of 15m.. These flows are all horizontal and the landscape is striking for its even skyline produced by flat topped plateaus and ridges that take off from them. They often carry small mesas and domal conical hills ('buttes') as around Sagar and Bina. Duricrust of laterite often cap the plateaus and ridges as around Sagar at 620 m.. The Amarkantak plateau is extensively capped by valuable bauxite at 1100 m.. Amphitheatrical valley heads

with narrow entrances and fairly steep side walls are fairly common along the edges of the plateaus and ridges. Extensive level plains and wide valley - flats complete the scenery.

The flat topped landforms in the area around Sagar were explained by West and Choubey (1964) as due to the operation of a pediplanation cycle during which the hill slope progressively retreated parallel to themselves without any vertical erosion (Fig.2.3). The mesas represent an intermediate stage in this retreat and the conical hills a near end stage. The stepped appearance on the slopes (in the northeastern part) is due to the differential rates at which this slope retreat is accomplished, the higher flows getting pushed back faster by lateral erosion over the tops of the lava flows than the lower ones. These hill slopes themselves have formed on the bedrock that weathers spheroidally at places, as in the sixth flow around Sagar which rest on an extensive plain, the spheroidal masses being over a meter in diameter. At other places, the whole slope may have formed on loose spheroidal boulders that are much smaller - a few tens of centimeters across as in the flows above the sixth, especially the eighth.

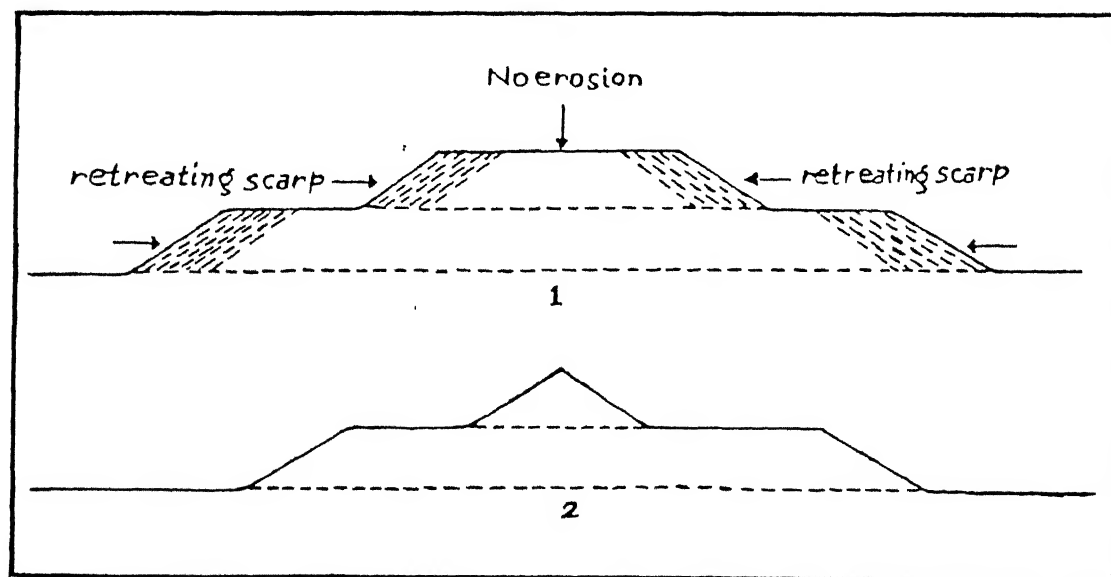


Fig. 2.3 Stages in the formation of a conical hill in the Deccan Trap by scarp retreat
(Source: West and Choubey, 1964)

The total absence of scarps in the northeastern part is due to vertical joints being almost completely absent (Subramanyan, 1981). The thickness of the soil profile varies inversely with the angle of slope, the gentler the slope, the thicker the profile. Likewise the distribution of certain species and communities of vegetation appears to be controlled by the slope. The absence of paleosols on any of the basaltic flows in this part and the presence of only weathering profiles on the flows clearly indicate that the flows were extruded in quick succession without allowing formation of soils (Subramanyan, 1981). The laterite and bauxite described earlier, however represent considerable period of still-stand during which continued weathering and attendant erosion resulted in the concentration of these oxides *in situ* towards the end of landscape cycles.

The Vindhyan topography is distinctly different from that of the Deccan traps. Unlike the Deccan traps, terracing is not a feature of the Vindhyan. The topography of the Vindhyan in the Sagar area is one that is characteristic of horizontal sedimentary rocks. Where the highest bed is a massive sandstone, the hills are fairly flat topped, The scarp slopes are steeper than those of the Deccan trap, and in places may be almost vertical above the scree slope. Being fairly pure quartzitic sandstones, the weathering is almost entirely mechanical, and erosion is greatly helped by the roots of trees penetrating the vertical joints and splitting the rocks apart.

In the vicinity of Sagar, the flat valleys between the Vindhyan hills are commonly partly filled with Deccan traps, and the complete profile of original pre Deccan trap valleys cannot be seen. But at Naryaoli, some 10 miles NW of Sagar, there occur two hills of Vindhyan, between which the village is situated. Here, for some distance around the hills,

the Deccan trap has been completely removed, and the original Vindhyan topography can be seen to consist of the steep scarp slopes surrounding the two hills, with a platform between and around the hills. This platform is not quite horizontal, slopping gently away from the scarps, and, unlike the horizontal Deccan trap platform, has been termed a pediment by West and Choubey (1964).

These authors have mentioned a further difference in topography between the two formations in Sagar area based on the slopes of the contours on the scarp slopes. In the case of the Vindhyan scarps, the contours are fairly smooth, with few indentations. The scarps are steep, in places approaching verticality, and there is little opportunity for streamlets to develop. But on the Deccan trap scarps the contours are indented by many little streams which unite lower to provide a dendritic pattern of drainage. As a result of this difference it is generally possible to tell from a study of the one inch topographical map, which hills are Vindhyan and which Deccan trap.

2.6.3 Drainage:

Narmada and Wainganga are the important rivers which originate on the basalts in the northeastern part. The Narmada commences on the Maikala Range at Amarkantak and the Wainganga rises on the Kurai plateau South of Seoni. The streams form a dendritic pattern and their network has a coarse to medium texture. Studying the detailed geomorphology of the country around Sagar, West and Choubey (1964), concluded that the present drainage, originating on a plateau of Deccan trap lavas which once covered the whole area, has been superimposed on the underlying Vindhyan rocks. Around Sagar, with the partial removal of the trap, a mature topography of the hills and valleys curved

out of horizontal Vindhyan have been resurrected. As a result, the new drainage pattern bears little relation to this pre-Deccan trap topography. The more powerful streams continued to erode in the courses they were following the Deccan trap, cutting gorges through the Vindhyan hills; but the weaker streams appear to be adapting their courses to old Vindhyan topography.

CHAPTER-3

METHODOLOGY

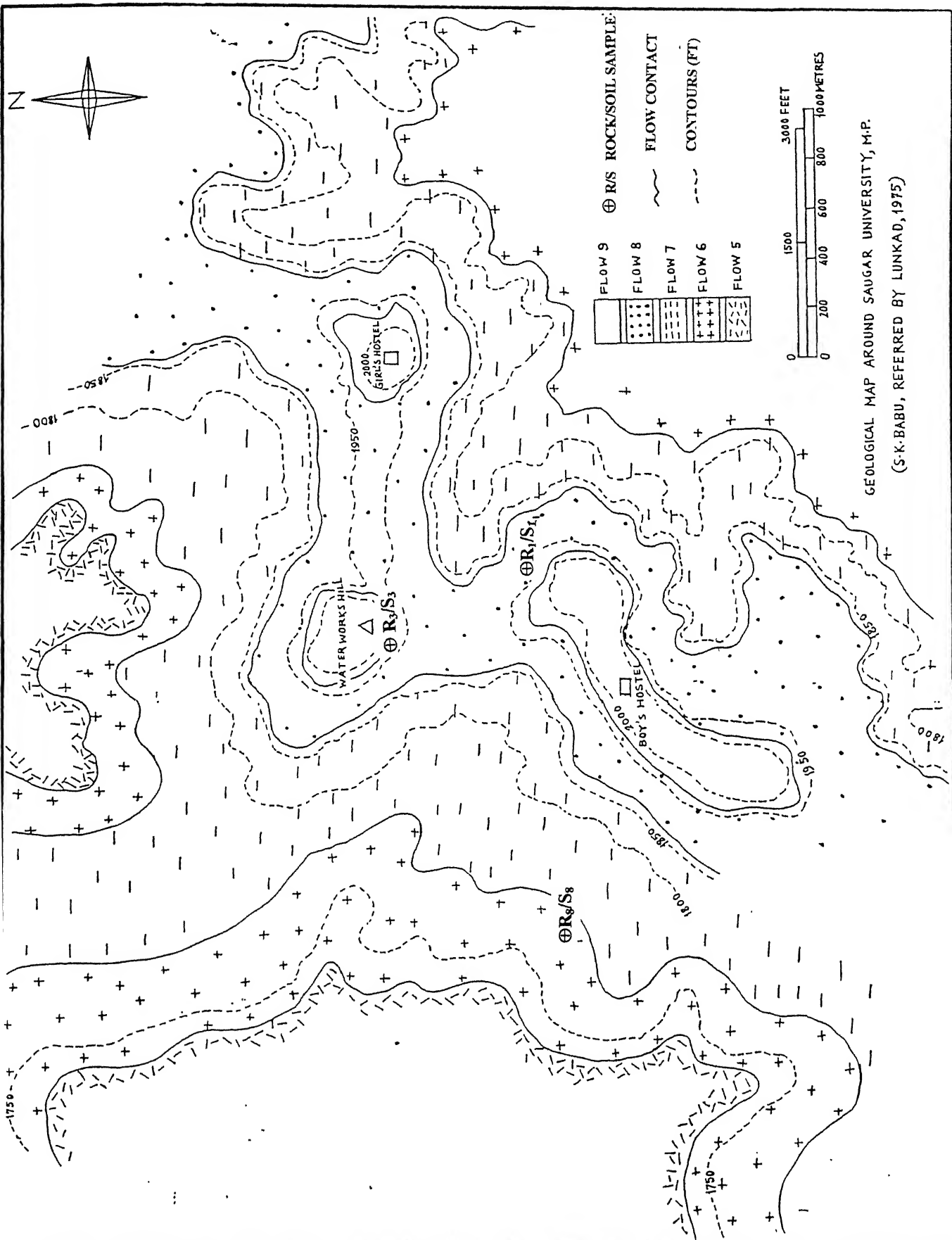
To achieve the objective of this thesis project the work was subdivided into three phases, namely, Field work, Laboratory work and Computer modeling. These are discussed below.

3.1 FIELD WORK:

The area of study is in and around Sagar University campus situated on the Malwa plateau in Madhya Pradesh. The field work was carried out in the month of May, 1996 to study the spheroidally weathered boulders and their weathering products from different flows exposed in this area. Representative samples of spheroidally weathered boulders, intermediate weathering products and soil samples were collected from four different flows (represented by R/S in Fig.3.1) covering the entire area, for subsequent laboratory study.

3.1.1 Location, Climate and Local Geology:

The area of study covers "Patharia Hill", which constitutes the highest hill of Sagar tehsil. Sagar town lies on Bina - Katni rail route, 75 km. east of Bina railway junction. The area around Sagar comprises undulating topography formed by Deccan trap flat topped hills and Vindhyan ridges. Patharia hill lies between latitude 23°49' and 23°50'N ; longitude 78°45'50" and 78°46'40"E in the Survey of India toposheet No. 55 I/13. Its elevation generally falls between 530 m. and 610 m. and at three places (Boys' hostel, Girls' hostel and Water Works) it exceeds 610 m.



GEOLOGICAL MAP AROUND SAGAR UNIVERSITY, M.P.
(S.K. BABU, REFERRED BY LUNKAD, 1975)

Fig. 3.1 Geological map around Sagar University campus showing location of sampling sites

The area falls under the tropical zone experiencing the monsoon type of climate. The period of June to September is the rainy season with average rainfall of 100-150 cm.. It is succeeded by winter commencing from October to February and temperature goes down to 15°C. The months of March to mid June constitute the Summer and the mercury may shoot up as high as 45°C. Relative humidity ranges from 20 to 40 % in the winter and 10 to 15 % in Summer.

The contrasting climate has important bearing on the weathering of the rocks of this area. During the rainy season, the rivers and streams are flooded, which erode and transport the material at a tremendous rate thereby exposing fresh rock surfaces for erosion. During other seasons, gravity, wind and vegetation act as agents of decomposition and disintegration, but the rate of weathering is negligible in comparison to what it is during rainy season.

The local geology of Patharia hill predominantly consists of Deccan traps with associated intertrappeans. Lateritic cappings occur sparsely and alluvium / soil is present on all the flows. There are four flows of the traps with two intertrappeans. These flows are designated as 1, 2, 3 and 4 in the ascending order. In the regional setup they are called 6th, 7th, 8th and 9th flows. The flows are horizontal and vary in thickness both laterally and vertically. The intertrappean between 1st and 2nd flows is fairly extensive, outcropping practically throughout the area of Patharia hill and also outside. The other occurring between 2nd and 3rd flows is of local nature. Intertrappeans comprise predominantly cherty limestone showing facies change to chert and clay.

Lateritic soil is found only at some places behind the University Rifle range and in Water Works hill between the flows 2nd and 3rd flows. Thin veneer of soil especially regur (Black Cotton Soil) is present on plain land. It is relatively thick on flow No.1 at the base of Patharia hill, occupied by the agricultural lands.

3.1.2 Sample Collection:

During the field work, most of the samples of rocks, intermediate weathering product and soils were collected from around Sagar University campus and some from quarry sites, a few kms. away from the University. The entire area is covered by four flows of basalt. They are demarcated on the basis of two surest field criteria, namely the break in slopes and the presence of intertrappeans. The flows also differ in their physical characters namely, colour, hardness, granularity, the way they break apart and the mode of weathering. The size of the boulders released due to weathering is an identifying characteristic, which is different from one flow to the other.

In and around Sagar University campus the spheroidally weathered boulders, loose and friable outer rindlets and soils from different flows were collected mostly from the road and other exposed sections. In quarry sites, complete profiles from fresh bedrock to the top soil were observed and samples were collected from different horizons.

3.2 LABORATORY WORK:

The samples collected in the field were of three types, namely, rock samples which are hard and tough, intermediate weathering product which are loose and friable and soil samples in powder form. They were studied by various methods described below.

3.2.1 Study of Rock Samples:

(i) In Hand-Specimens

Weathering rind morphology, appearance of weathered rock, grain size, colour, mineralogy and texture were characterised in the naked eye and with the help of *Bausch and Lomb (USA)* binocular microscope.

(ii) In Thin Sections

The thin sections of rock samples were studied under the optical microscope *Leitz, LABORLUX 11 POLS (Leitz Wetzlar, Germany 553 428)*, under varying magnification which helped in identifying the constituent minerals of weathered boulders and the alterations at their surfaces. The properties like, colour, shape, cleavage pattern, extinction angle, twinning and interference colour were used for this purpose.

(iii) X-ray Diffraction Analyses

The X-ray diffraction analyses were made to establish the reactant and product mineralogy in fresh rock and its alteration products. For X-ray diffraction the bulk powder of fresh rock and weathered rindlets were prepared with the help of a mortar and pestle. Oriented slides were prepared by depositing a suspension on glass slide. All the bulk powder and oriented slide samples were scanned under X-ray diffractometer *Model ISO - DEBYFLEX 1001 and 1002 of RICH. SEIFERT and Co.* at 20 mA, 30 KV using $\text{CrK}\alpha$ and $\text{CuK}\alpha$ radiation with monochromator.

(iv) Electron Microprobe Analyses

The geochemical changes across the core-rim interface of spheroidally weathered boulders were studied with a *JEOL Model JXA-8600 MX* Electron Microprobe, with beam parameters 15.0 KV and 2.48×10^{-8} amp to document weathering process on the smaller scale of grain-size alteration. X-ray mapping was done along a line across the interface of fresh rock core and weathered rim of a 2.5 cm. polished, silver coated rock chip, to study the elemental distribution across this interface.

(v) Scanning Electron Microscopy

To study the variation in elemental concentration across the interface of fresh rock core and weathered rim, Energy Dispersive X-ray Analysis (EDX) was carried out on a *JEOL Model JSM 840A* Scanning Electron Microscope with an Energy Dispersive Spectrometer (EDX) attachment of *KEVEX (USA)*. 2.5 cm. polished rock chip was coated with gold-palladium coating in vacuum to make it conductive.

3.2.2 Study of Soil Samples:

(i) X-ray Diffraction Analyses

The soil samples were first separated from roots, stems etc.. After cleaning the samples, they were passed through different sieves to collect samples of controlled grain size for further analysis. Oriented slides were prepared by depositing a suspension on a glass slide. This enhanced the low angle basal peaks of flaky minerals like clays. To establish the mineralogy of weathering products, bulk and oriented slides of soils were run in X-ray diffractometer of earlier mentioned model and specifications. Slow scanning was adopted to resolve doublets and shoulders on peaks.

(ii) Scanning Electron Microscopy

Shapes and morphology of minerals in intermediate weathering products and soils were observed under the Scanning Electron Microscope of the above mentioned model. Fine powdered samples of soils and outermost rindlets were poured into an acetone solution and then ultrasonicated for fifteen minutes. The samples were then oven dried at nearly 80°C and put into a specimen stub with the help of micropipet. To make the samples conductive, they were coated with gold-palladium coating in vacuum.

3.3 COMPUTER BASED MODEL:

In the present study, the volume change due to weathering of constituent minerals in basalt is considered to be responsible for the inbuilt stress leading to spheroidal weathering. In order to quantify this aspect, a computer based three mineral model was developed in C - Language on an HP-9000 system. In this model, starting with the modal volume percentage of plagioclase, augite and magnetite in fresh rock of four different flows, successive iterations have been made for different combinations of weathering reactions and proportions of alteration to calculate the net volume change.

CHAPTER-4

RESULTS AND DISCUSSION

To meet the objective of this thesis work, representative samples of spheroidally weathered boulders and their weathering products were collected from different basalt flows mentioned in the preceding chapter. Subsequent laboratory work was carried out on these samples to ascertain the overall mechanism of spheroidal weathering in basaltic rock. The different basalt flows occurring around Sagar University campus are described first.

4.1 DESCRIPTION OF THE FLOWS:

The geological map of the area around Sagar University campus has been shown in Fig. 3.1. Megascopically all the flows look alike with some minor variations. They are generally light to dark steel grey, black brownish and greenish grey in colour. Spherical vesicles of variable diameter are observed in the samples of all the flows. Occasionally they are filled by secondary cryptocrystalline silica (chalcedony), some green minerals and zeolite. Lower flows are coarser grained, having more widely spaced cooling cracks that have given rise to spheroids of relatively larger size. As compared to the lower flows, the upper flows are relatively fine grained, compact, hard and tough with freshly fractured surfaces. Columnar joints in the flows are common. Limonitic stain of different shades of yellow are seen on the weathered boulders. The other field characters of the individual flows are as follows:

4.1.1 6th Flow

As mentioned in the previous chapter, this flow is the lowest horizon at this locality. This flow is exposed between approximate elevations of 520 to 535 m.. Some

exposed sections of this flow were observed near the University hockey ground (R₈/S₈ in Fig. 3.1). It breaks when struck by hammer and it occurs as medium sized boulders with calcareous coating. The flow shows associated abundant kankar nodules. Hence there must have been original gas cavities or vesicles which are now filled with calcite. The flow shows spheroidal weathering with change to onion skin shells in the upper parts. At places some whitish clay horizons are present in the weathering profile. Thin veneer of black cotton soil cover the top of this flow.

4.1.2 7th Flow

This flow occurs between approximate elevations of 535 to 550 m.. It contains large boulders with rough feel due to differential weathering (Plate 4.1). It is relatively coarse grained with occasional microlaths of plagioclase phenocrysts. Exposures were observed in the road section between University Library and University playground.



Plate 4.1 Large spheroidally weathered boulders with a number of rindlets. 7th flow, Road section between University Library and Playground, Sagar

4.1.3 8th Flow

Occurring between approximate elevations of 550 to 585 m., it is characterized by medium to small sized boulders. This flow is exposed behind the University Campus Rifle Range (R_1/S_1 in Fig. 3.1). The top of the flow is full of vugs and vesicles. It is fine grained with limonitic stain and shows onion skin shells. This flow is covered by reddish-brown lateritic soil (Plate 4.2).

4.1.4 9th Flow

With the top being eroded, presently it is exposed between approximate elevations of 585 to 620 m.. It is dark steel grey in colour, extremely fine grained with vesicles at the top filled with secondary green earth materials. This flow is bouldery in occurrence with decrease in size of boulders with height. These boulders are very hard, tough and rich in iron-oxide. Limonitic stains of different shades of yellow were seen on weathered boulders. Its contact with lower (8th) flow is scoured and shows development of zeolites at places. The flow is well exposed behind the Applied Geology department, Water Works hill (Plate 4.3).

4.2 MINERALOGICAL AND TEXTURAL STUDIES:

Mineralogical and textural studies of the samples collected from different flows were carried out through visual observations, under binocular microscope and mostly from X-ray diffraction pattern. In addition, some thin sections of the samples were also studied under optical microscope.

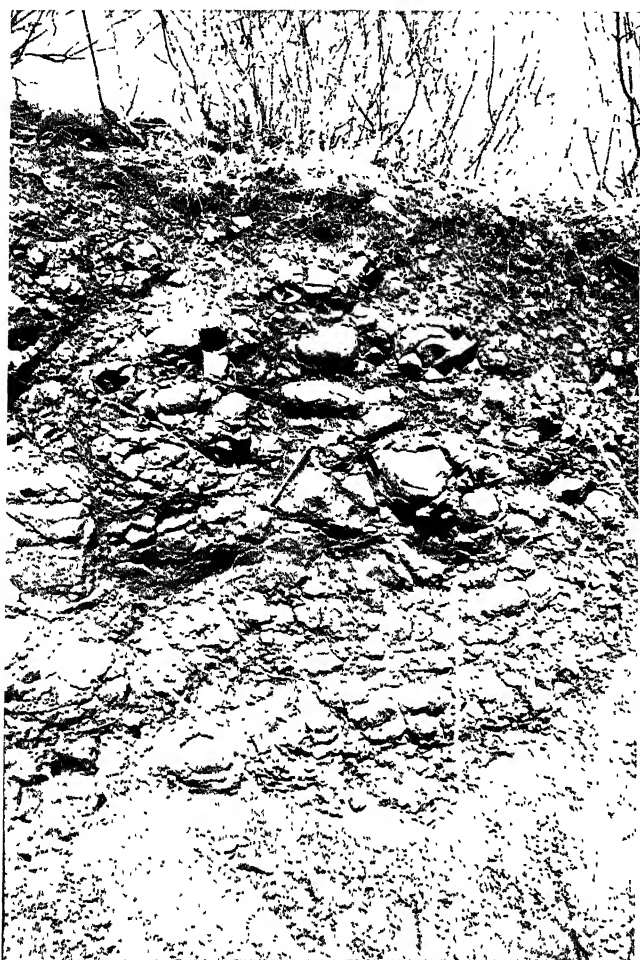


Plate 4.2 Profile showing spheroidal weathering and reddish brown top soil. 8th flow, behind University Campus Rifle Range, Sagar



Plate 4.3 Spheroidal weathering profile from 9th flow , behind Applied Geology Deptt., Water Works hill, Sagar University Campus

4.2.1 Fresh Rock Core:

The fresh rock core typically has a porphyritic texture with phenocrysts of plagioclase, and less frequently of pyroxene in a matrix containing fine grained plagioclase, pyroxene and partly devitrified glass. Plagioclase phenocrysts occur as sub-hedral to euhedral crystal with a tendency to form clusters. They show simple, parallel and complex twins. As compared to plagioclase, pyroxene phenocrysts are sparse and are represented by pale-brown, non pleochroic augite. Sometimes this augite shows sub-ophitic to intergranular relationship with the plagioclase and occurs as fresh, short prismatic or squarish crystals with good cleavage. The dominant opaque mineral is magnetite, which is commonly disseminated throughout the groundmass. It occurs as granular, square and rectangular crystals, elongated bars and also in irregular patches. Glass is present in the interstices of groundmass crystals. Its colour is varied - red, orange, yellow and brownish black.

The feldspar was identified to be a calcic-plagioclase from its X-ray peaks (Table 4.1) and optical properties. From twinned feldspar laths in the thin section, the extinction angle with respect to the (010) twin plane was measured to be around 25.8° . This corresponds to plagioclase of An_{85} composition according to the determinative graph given by Wahlstorm (1955). Mineralogically, plagioclase with An_{70} to An_{90} composition is named bytownite.

The other X-ray peaks observed (Table 4.1) matched with the pyroxene of augite composition and magnetite. Magnetite was confirmed by magnetic property of black particles in rock powder.

TABLE 4.1 Identification of minerals in fresh rock (core) by comparison with standard mineral X-ray peaks (\AA)

Observed	Augite	Plagioclase(An_{77})	Magnetite	Quartz
4.03		4.030		
3.79		3.748		
3.60		3.624		
3.42		3.459		
3.34				3.340
3.19		3.196		
2.99	2.990		2.970	
2.94	2.940	2.950		
2.83	2.860			
2.59	2.560			
2.53			2.530	

Besides the above mentioned minerals, small proportion of quartz is also present in the fresh rock core. Quartz was identified by its characteristic 3.34\AA X-ray peak and also from thin section observation. The X-ray diffraction pattern in Cu radiation of fresh rock core from 9th flow (R_3/S_3 in Fig 3.1) is shown in Fig.4.1. A similar pattern in Cr radiation contained higher angle peaks of augite and magnetite at 2.83 , 2.53 and 1.49\AA .

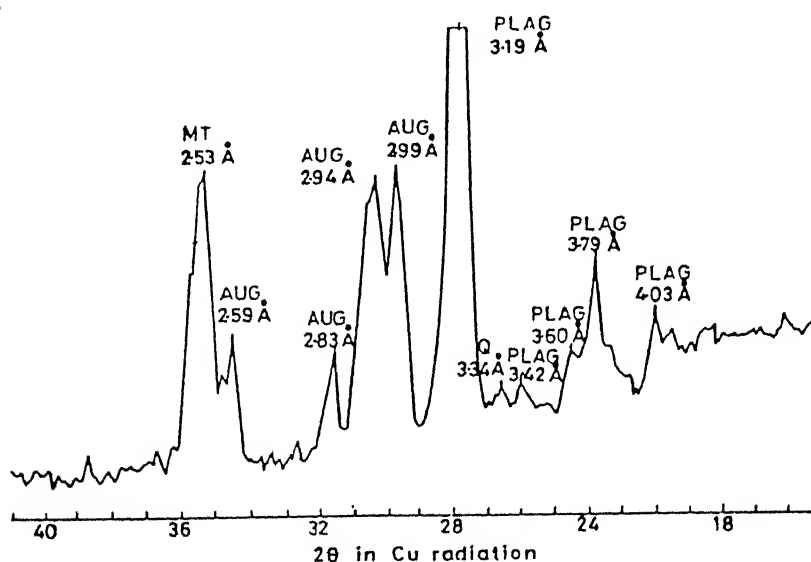


Fig. 4.1 XRD pattern of fresh rock core

4.2.2 Intermediate Weathering Product:

The innermost rindlets, immediately adjacent to the fresh rock core, retain nearly the same mineralogy and texture as the fresh rock core. These rindlets are compact, indurated and handspecimen shows reddish-brown iron-oxide stain on the surface (Plate 4.4).

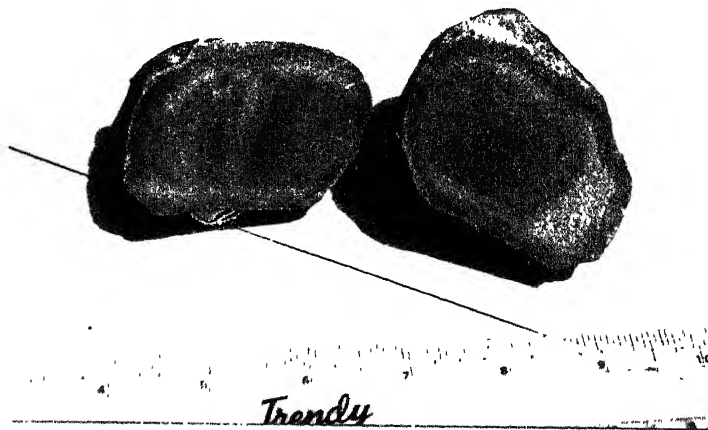


Plate 4.4 Spheroidally weathered boulders from 9th flow, Sagar, showing fresh rock core and innermost rindlet with reddish brown iron oxide stain on the surface

(photo: Dr. Rajiv Sinha)

Thin section of one such rindlet from spheroidally weathered boulder of 9th flow (R_3/S_3 in Fig.3.1) showed the presence of plagioclase, pyroxene, magnetite and interstitial glass. However, here the minerals are partly altered. Twinning planes and grain boundaries are partially obscured by clay minerals. Frequent cloudiness of plagioclase is due to the formation of clay. Plagioclase alteration to clay minerals along minute solution channels and along grain boundaries was visible in the thin section (Plate 4.5). Mafic minerals are sometimes so intensely Fe-stained that their cleavage planes, as well as their grain

boundaries are often obscured. This is because iron (Fe^{+2}) liberated from the lattice sites of these minerals is oxidized in the weathering front and insoluble Fe^{+3} is precipitated as amorphous limonite or goethite.

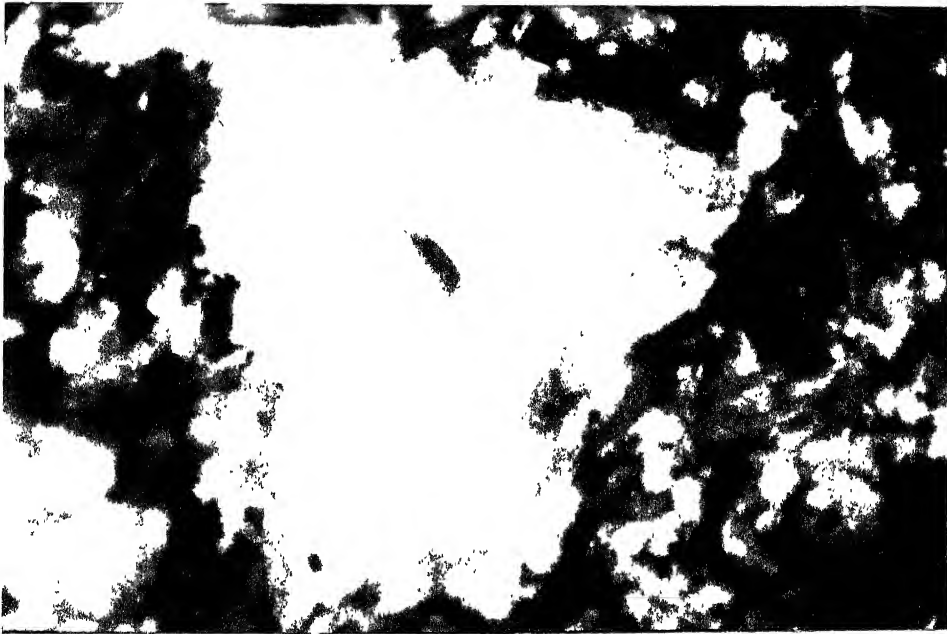


Plate 4.5 Photomicrograph showing alteration of plagioclase to clay along solution channels and grain boundaries. One augite grain (right bottom corner) shows limonitic stain around grain boundary. Innermost rindlet, 9th flow, Water Works hill, Sagar (crossed nicol, 120X)

A thin section made across the visually-identified boundary (interface) between the fresh rock core and innermost rindlet showed that plagioclase and pyroxene grains are altered in the innermost rindlet. Size of the phenocrysts are smaller in this rindlet and grain boundaries are irregular, whereas, the phenocrysts in the core are coarser and show regular grain boundaries (Plate 4.6).

X-ray diffraction pattern (Fig.4.2) of the powders of bulk samples confirmed the above mentioned minerals (Table 4.2). Besides plagioclase, augite and quartz, a partly hydrated halloysite (modified kaolinite) was identified from its 7.40\AA basal peak.

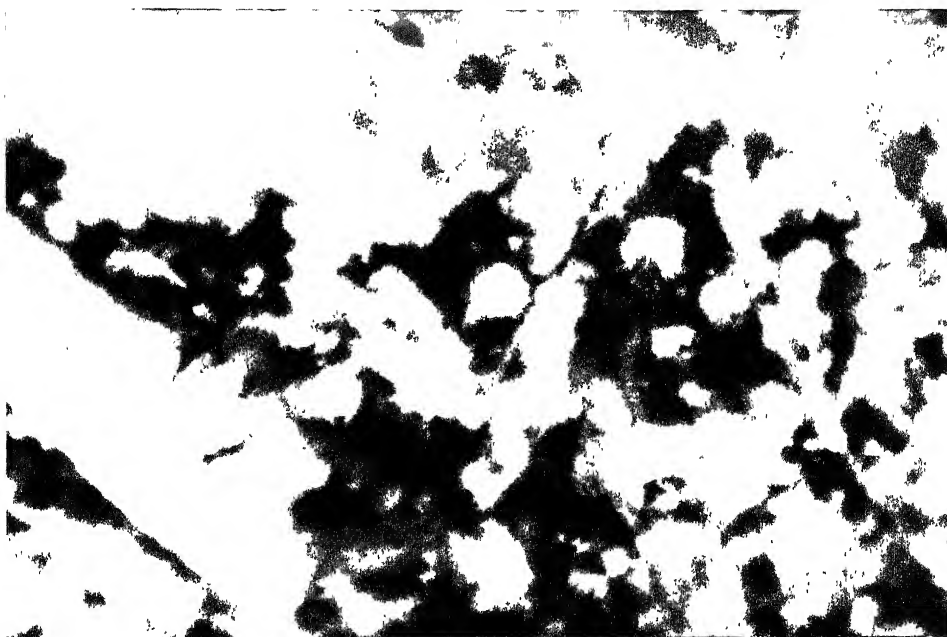


Plate 4.6 Photomicrograph of the interface of fresh rock core (left) and innermost partially altered rindlet (right) showing the difference in appearance of plagioclase grains. 9th flow, Water Works hill, Sagar (crossed nicol, 120X)

TABLE 4.2 Identification of minerals in partly weathered compact innermost rindlet by comparison with standard mineral X-ray peaks (\AA)

Observed	Augite	Plagioclase(An_{77})	Halloysite	Quartz
7.40			7.410	
6.51		6.520		
4.69		4.690		
4.25				4.250
4.03		4.030		
3.88		3.888		
3.74		3.748		
3.45		3.459		
3.34		3.357		3.340
3.19		3.196		
2.99	2.990			
2.94	2.940			
2.91	2.860			
2.57	2.560			
2.51	2.510	2.504		

The intense reddish-brown colouration around and within the mafic minerals indicate the presence of ferric iron, majority of which can be accounted for only as goethite or as an amorphous phase (Plate 4.4).

Mineralogical similarity with fresh rock core and poorly crystalline nature of most of the secondary weathering products indicate that these innermost rindlets represent the incipient alteration stage.

Slightly more advanced stage of weathering was detectable in the non-indurated, friable outermost rindlets. These rindlets have lost their physical coherence with the fresh rock core. Some of these rindlets can even be broken with one's fingers. In handspecimens, powder of these loose incoherent rindlets shows slightly whitish colour, which may be due to the presence of clay minerals. X-ray diffraction pattern (Fig.4.3 and Table 4.3) of the powder of such an outermost rindlet from 9th flow (R_3/S_3 in Fig.3.1) show almost the same mineralogy as that of the previously described innermost rindlets. Here halloysite shows its characteristic 4.46 \AA peak in addition to the basal peak at 7.36 \AA . Its presence was further confirmed from its typical tubular morphology in the scanning electron micrograph (Plate 4.7). From visual observations and X-ray diffraction pattern it seems that these outermost rindlets represent a more advanced stage of weathering.

4.2.3 Final Weathering Product:

The ultimate product of weathering is soil. As mentioned in the previous chapter, two types of residual soils develop by weathering of Deccan basalt. Low grounds are generally covered by thick clayey loam - the black cotton soil or regur. This is dark grey to

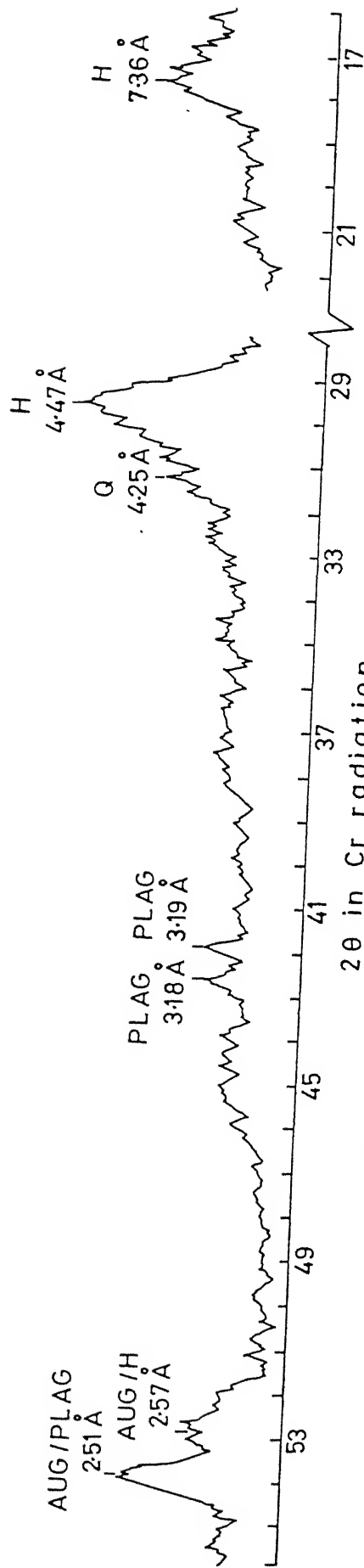


Fig. 4 3 XRD pattern of partly weathered outermost rindlets

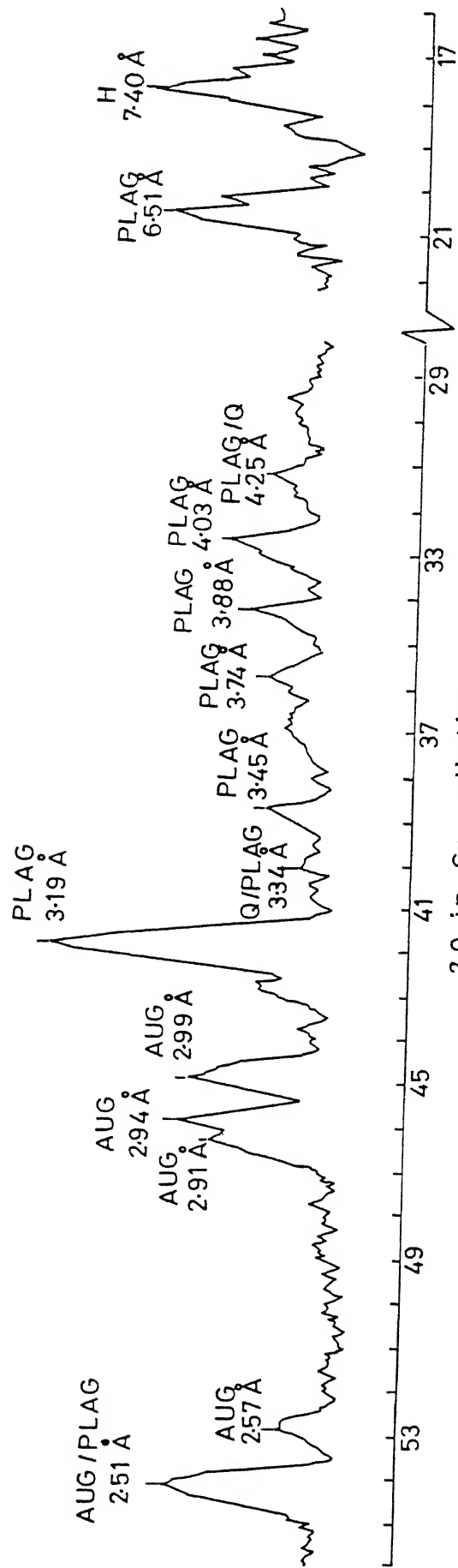


Fig. 4 2 XRD pattern of partly weathered compact innermost rindlet

TABLE 4.3 Identification of minerals in partly weathered outermost rindlets by comparison with standard mineral X-ray peaks (\AA)

Observed	Augite	Plagioclase(An_{77})	Halloysite	Quartz
7.36			7.410	
4.47			4.460	
4.25				4.250
3.19		3.196		
3.18		3.170		
2.57	2.560		2.560	
2.51	2.510	2.504		

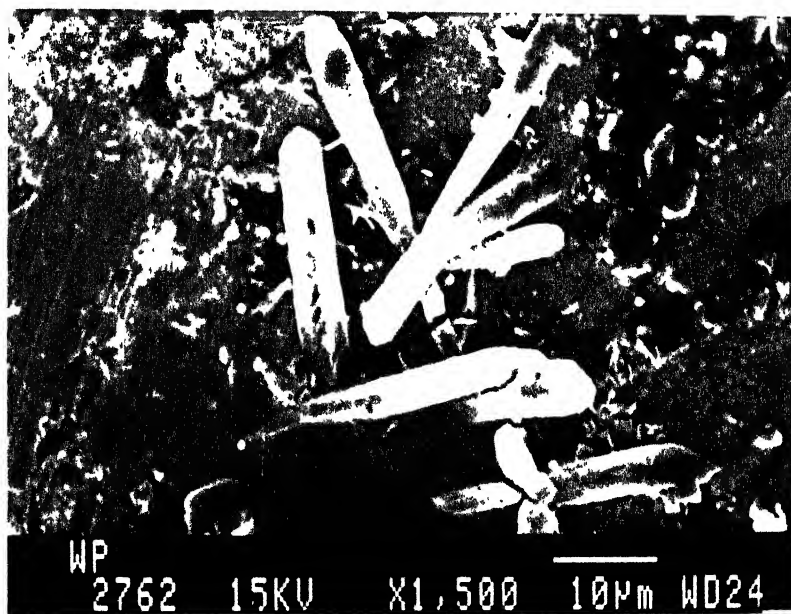


Plate 4.7 Scanning electron micrograph showing typical tubular morphology of Halloysite in weathered outermost rindlets. 9th flow, Water Works hill, Sagar

black in colour, very sticky when wet and cracks easily on drying. Hill tops and plateaus are covered by thin reddish-brown lateritic soil.

X-ray diffraction pattern for oriented slides of these reddish-brown soil from 9th flow (R_3/S_3 in Fig.3.1) shows the presence of plagioclase, augite, quartz, halloysite and a mineral of smectite group (Table 4.4). Halloysite was identified from its broad X-ray peak at around 7.32 to 7.74 \AA (Fig. 4.4) and the tubular morphology in scanning electron micrograph. Smectite group of mineral was identified to be a Ca-beidellite from its X-ray peaks at around 15 \AA and 4.46 \AA . The high intensity of the peak at around 4.46 \AA is due to the overlapping of beidellite and halloysite peaks. The X-ray diffraction pattern for the oriented slides of reddish-brown soil from 8th flow (R_1/S_1 in Fig.3.1) did not show the presence of beidellite, however, the other minerals plagioclase, augite, quartz and halloysite were present.

TABLE 4.4 Identification of minerals in Red Soil (9th flow) by comparison with standard mineral X-ray peaks (\AA)

Observed	Beidellite	Halloysite	Plagioclase(An_{77})	Augite	Quartz
14.28 15.27	14.0 - 15.0				
7.32 7.48 7.74		7.20 - 7.50			
4.48 4.42 4.36	4.46	4.46			
3.76			3.748		
3.34					3.34
3.19			3.196		
2.51	2.50		2.504	2.51	

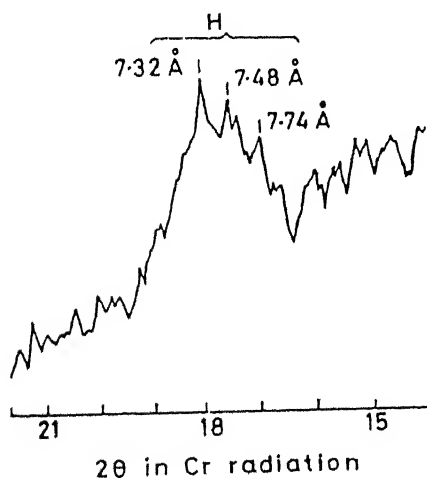


Fig. 4.4 XRD pattern of Red Soil from 9th flow showing Halloysite peaks

The X-ray diffraction pattern of black cotton soil from 6th flow (R_8/S_8 in Fig.3.1) showed the presence of beidellite, augite, plagioclase and quartz (Table 4.5). beidellite showed a characteristic basal peak at 14.59\AA in oriented slides which expanded to $18.24 - 19.89\text{\AA}$ after glycolation (Fig.4 5). There are some shoulders in the basal peak which may be due to the presence of mixed layer clays.

TABLE 4.5 Identification of minerals in Black Cotton Soil (6th flow) by comparison with standard mineral X-ray peaks (\AA)

Observed	Beidellite	Plagioclase(An_{77})	Augite	Quartz
14.28 15.27	14.0 - 15.0			
4.39 4.48	4.46			
3.81		3.748		
3.34				3.34
3.19		3.196		
2.94			2.94	
2.51			2.51	

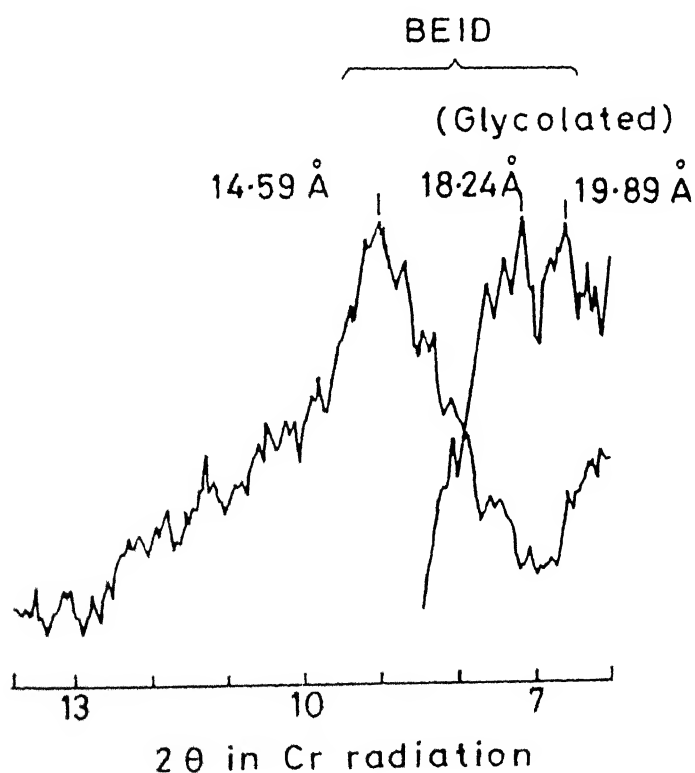


Fig. 4.5 XRD pattern of Black Cotton Soil from 6th flow showing glycol expansive Beidellite peaks

The presence of primary minerals like plagioclase, pyroxene and quartz in the weathering products indicates that decomposition was incomplete and these are residual after weathering.

Table 4.6 summarizes the results of the mineralogical and textural studies, discussed so far.

TABLE 4.6 Mineralogy of samples collected from different locations

Sample Locations	Nature of Samples	Mineralogy
R ₃ /S ₃ (9th flow)	Fresh rock core in spheroidally weathered boulders	Ca-Plagioclase, Augite, Magnetite, Quartz
R ₃ /S ₃ (9th flow)	Indurated, compact innermost rindlet in the immediate vicinity of fresh rock core	Ca-Plagioclase, Augite, Halloysite, Quartz, Fe-oxide (Goethite?)
	Non indurated, friable outermost rindlets	Ca-Plagioclase, Augite, Halloysite, Quartz
R ₁ /S ₁ (8th flow)	Reddish-brown lateritic soil	Ca-plagioclase, Augite, Quartz, Halloysite, Fe-oxide (Goethite?)
R ₈ /S ₈ (6th flow)	Black - Cotton soil	Ca-Plagioclase, Augite, Beidellite, Quartz

4.3 GEOCHEMICAL CHANGES ACROSS THE CORE-RIM INTERFACE:

The spheroidally weathered boulders collected from the study area has a typical morphology of onion-skin layers surrounding a core of fresh rock. A section cut through the boulder shows several coloured zones, starting with a dense black core and grey to brown zones towards the rim (Plate 4.4). Augustithis and Ottemann (1966) compared the mineralogy and X-ray fluorescence (XRF) spectra of such zones and explained their origin by diffusion and migration of elements during weathering. A similar approach has been adopted in the present work using microanalytical techniques like (I) X-ray mapping under

electron probe microanalyzer (EPMA) and (ii) energy dispersive X-ray analysis attached to scanning electron microscope (SEM-EDX).

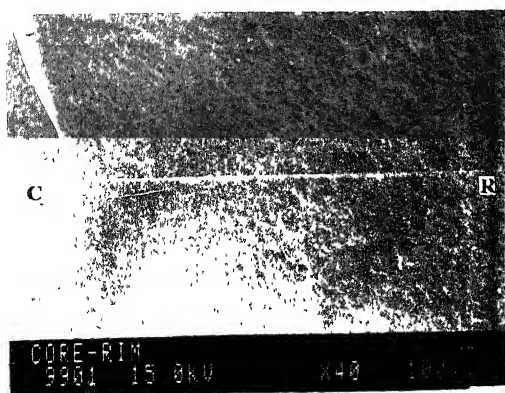
X-ray mapping along a line (Plate 4.8 a) across the interface of fresh rock core and rim shows the elemental variation illustrated in Plate 4.8b to 4.8f . It is clear that Fe and Ca are enriched towards the rim (right of the photographs), whereas, Si, Al and Mg are enriched towards the core (left of the photographs). However, the image of Ca is not very prominent. These trends have a broad similarity with the chemical analysis given by Augustithis and Vgenopoulos (1983). A part of their data is shown in Table 4.7.

TABLE 4.7 Basalt (spheroidally weathered) Phutkapahar, Central India. Modified after Augustithis and Vgenopoulos, 1983.

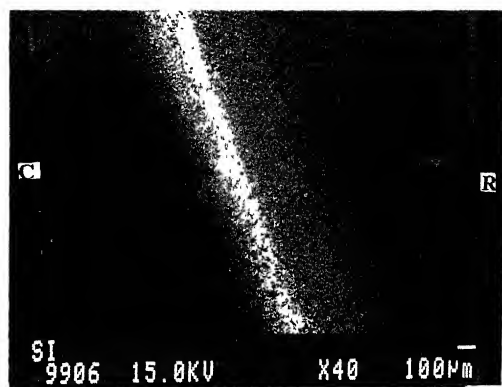
	SiO ₂	Al ₂ O ₃	Fe ₂ O ₃	CaO	MgO
Zone I	46.4	16.4	14.2	7.2	9.5
Zone II	51.6	10.6	18.7	9.2	5.6
Zone III	25.0	15.5	38.8	9.2	4.5

Here zone I represents the core while zone II and zone III are the intermediate diffusion ring and the alteration margin respectively. It is seen that Fe₂O₃ and CaO increase towards the rim, whereas SiO₂, Al₂O₃ and MgO show a general decrease from core to rim.

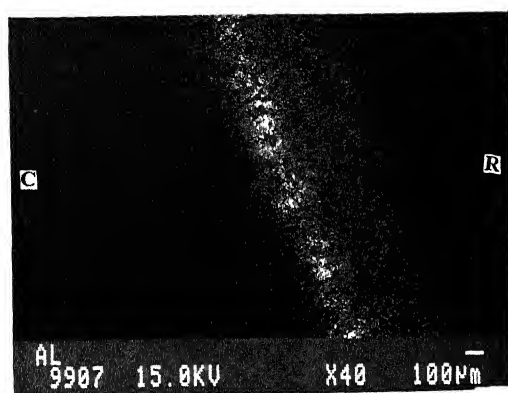
The SEM-EDX obtained across the core-rim interface shows a pattern roughly similar with the EPMA results. Here also Fe shows a continuous increase from core towards rim, whereas, Si, Al and Mg decrease from interface towards the rim. However Ca shows a different trend compared to the EPMA data because there is a slight decrease between the interface and the rim (Fig. 4.6).



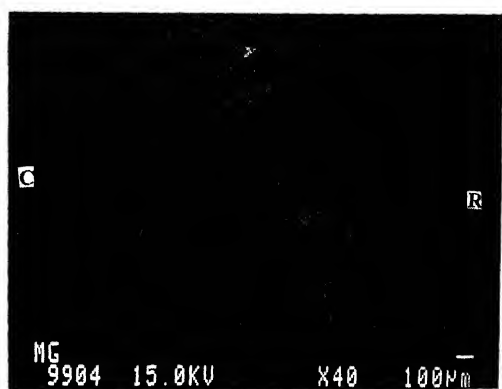
(a)



(b)



(c)



(d)



(e)



(f)

Plate 4.8 X-ray mapping under EPMA across core-rim interface showing: (a) scan line and variation of (b) Si, (c) Al, (d) Mg, (e) Fe and (f) Ca.
c-Core, r-Rim

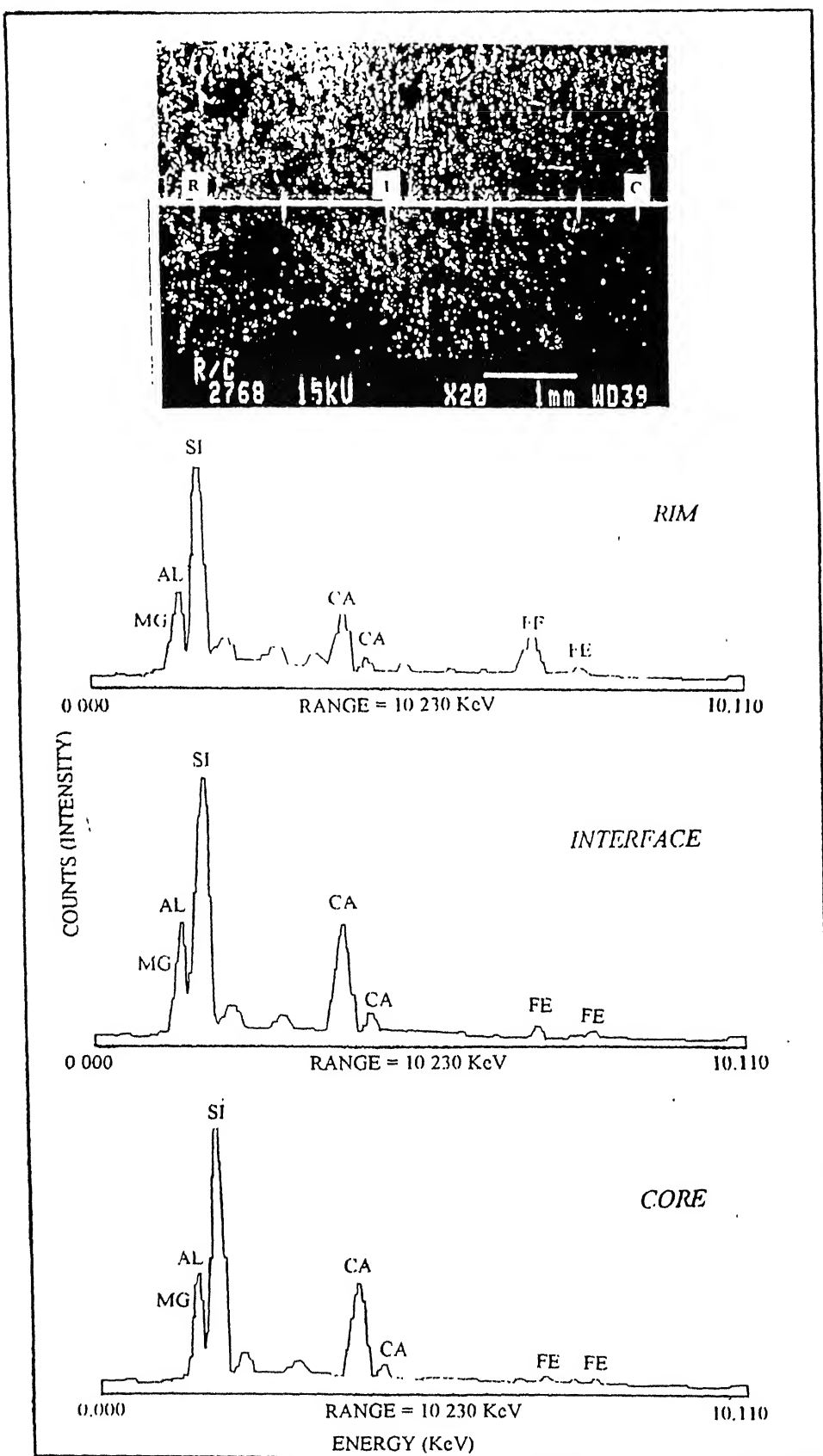


Fig. 4.6 SEM-EDX across the core-rim interface, 9th flow Basalt

Enrichment of iron towards the rim as discussed above is likely to be due to the formation of iron-oxide by reprecipitation of leached iron. The higher proportion of Si, Mg and Al in the so called leached zone (Augustithis and Ottemann, 1966) can be due to a residual concentration of aluminosilicate minerals like halloysite and smectite. The pattern of Ca cannot be clearly explained due to some ambiguity in data as discussed above. On the other hand, the calcium phases likely to occur in the weathering zone are a Ca-beidellite or calcite (not confirmed during the study, but reported as weathering product of Ca-plagioclase by Fritz and Mohr, 1984).

The progressive alteration during weathering is accompanied by development of solution channels or microcracks which commence from the periphery and advance towards the centre of fresh rock mass. These solution channels or microcracks play a major role in leaching and migration of elements as discussed by several authors (e.g. Fritz and Ragland, 1980; Fritz and Mohr, 1984; Fritz, 1985).

4.4 Volume Change During Weathering Reactions:

The existing literature clearly indicates that the stress responsible for the development of onion-skin shells on spheroidally weathered boulders is generated inside the rock mass. The underlying process is chemical weathering, in which the secondary minerals produced by weathering occupy a volume larger than that of the primary minerals. Therefore, different standard techniques like X-ray diffraction, optical and scanning electron microscopy were adopted to identify the primary and secondary minerals present in the spheroidally weathered Deccan basalt boulders from the Sagar area. The next step obviously is to formulate the appropriate weathering reactions which will result

in a net volume increase during the decay of primary minerals to an assemblage of secondary minerals in the weathering product.

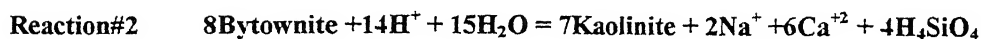
The present results indicate the presence of three major primary minerals in the Deccan basalt of Sagar area. These are (1) a calcic plagioclase of bytownite type. There is some ambiguity about its exact composition. Although the X-ray peaks match with those of An₇₇ phase, the extinction angle of a few twin lamellae indicate a higher Ca content around An₈₅. On the other hand Najafi et al (1981) have reported plagioclase in Deccan basalt upto An₇₃ composition and Durge (1987) has reported plagioclase of labradorite / bytownite (An₆₀ - An₇₀) variety from the study area. In order to select a composition within the above range and also for convenience of balancing chemical reactions, an idealized formula of bytownite An₇₅ i.e. $\text{Na}_{0.25}\text{Ca}_{0.75}\text{Al}_{1.75}\text{Si}_{2.25}\text{O}_8$, has been used in the present study, (2) a pyroxene of augite variety with idealized formula, $\text{CaMgFeAl}_2\text{Si}_3\text{O}_{12}$ and (3) Magnetite, Fe_3O_4 . It turns out that these minerals are highly weatherable according to geochemical concepts, e.g., the Goldich Weatherability Series (Krauskopf, 1982). The clay minerals which are produced from the above primary minerals are identified as halloysite belonging to the kaolinite group, and beidellite belonging to the smectite group. Their chemical composition have been idealized as $\text{Al}_2\text{Si}_2\text{O}_5(\text{OH})_4$ and $\text{Ca}_{0.17}\text{Al}_{2.33}\text{Si}_{3.67}\text{O}_{10}(\text{OH})_2$. There is conspicuous iron staining on the outer rindlets of the spheroidally weathered boulders and the reddish-brown soil obviously contains iron-oxide. However, no X-ray peak of the mineral goethite (which is the commonly reported mineral in this environment) could be detected in the samples. This could be due to relatively small proportion as well as the poorly crystalline nature of freshly precipitated iron-oxide.

Moreover, SEM of reddish-brown soil showed clusters of needle shaped crystals which needs further identification as goethite. Therefore, the formula of goethite, FeO.OH has been used to represent the reddish-brown layers in the weathering zone.

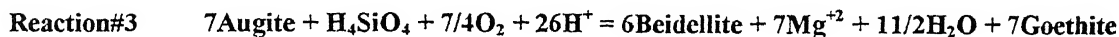
Based on the above mineralogy of reactants and products during weathering of Deccan basalt in the Sagar area, the following five representative reactions have been formulated.



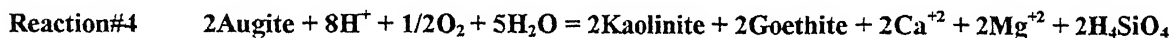
(Dissolved silica)



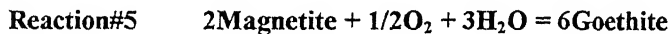
(Dissolved Silica)



(Dissolved Silica)



(Dissolved Silica)



Percent change in molar volume of these minerals during reaction was calculated in the following way:

In the reaction of Bytownite weathering to Beidellite (Reaction#1),

$$\text{Molar volume of Bytownite (VBy)} = \frac{\text{Molecular weight}}{\text{Specific gravity}} = \frac{274.22}{2.72} = 100.81\text{cc}$$

$$\text{Molar volume of Beidellite (VBa)} = \frac{366.64}{2.60} = 141.01\text{cc}$$

4 moles of Bytownite weathers to form 3 moles of Beidellite

$$\begin{aligned}\text{therefore, change in molar volume } (\Delta V\%) &= \frac{3VBd - 4VBy}{4VBy} \times 100 \\ &= \frac{423.03 - 403.24}{403.24} \times 100 \\ &= 4.9\%\end{aligned}$$

Similar calculation of ($\Delta V\%$) for other reactions have been listed in Table 4.8

TABLE 4.8 ($\Delta V\%$) values for different reactions

Reactions		($\Delta V\%$)
Reaction#1	4Bytownite \rightarrow 3Beidellite	+4.90
Reaction#2	8Bytownite \rightarrow 7Kaolinite	-13.81
Reaction#3	7Augite \rightarrow 6Beidellite + 7Goethite	+6.91
Reaction#4	2Augite \rightarrow 2Kaolinite + 2Goethite	-9.35
Reaction#5	2Magnetite \rightarrow 6Goethite	+40.09

This table clearly shows that the volume expansion during weathering of rock forming minerals depends on the assemblage of secondary minerals. In other words, an increase in volume cannot be generalized for all reactions representing the formation of clay minerals from plagioclase and augite. This is because ($\Delta V\%$) is positive for Reaction#1, Reaction#3 and Reaction#5, whereas it is negative for Reaction#2 and Reaction#4.

To quantify the appropriate combination of these five simultaneous reactions, which will result in a net positive ΔV essential for spheroidal weathering, a simplified three mineral model was developed as discussed below.

4.5 THREE MINERAL COMPUTER MODEL:

The computer program was written in C - language on an HP-9000 system. Starting with the modal volume (%) of bytownite, augite and magnetite in fresh rock of four different flows, successive iterations have been made for different combinations of weathering reactions and proportion of alteration of individual minerals. The data of Durge (1987), on modal volumes (%) of three primary minerals for the four different flows of Sagar area have been recalculated to hundred after neglecting the minor constituents and used in this model.

The computer program and different abbreviations used in this model is supplied in appendix-II. The output of the program is given in Table 4.9. A schematic flow diagram of the model is shown in Fig.4.7.

The steps of iteration consisted of calculation of net $\Delta V(\%)$ for weathering of a particular flow, keeping the original modal composition (V_{11} , V_{22} and V_{33}) of three primary minerals and alteration fractions (a_1 , a_2 and a_3) constant and varying the proportion of different reactions (x , y and z). This calculation has been repeated for the other sets of values of a_1 , a_2 and a_3 for the same flow, as well as for similar combinations for all the flows.

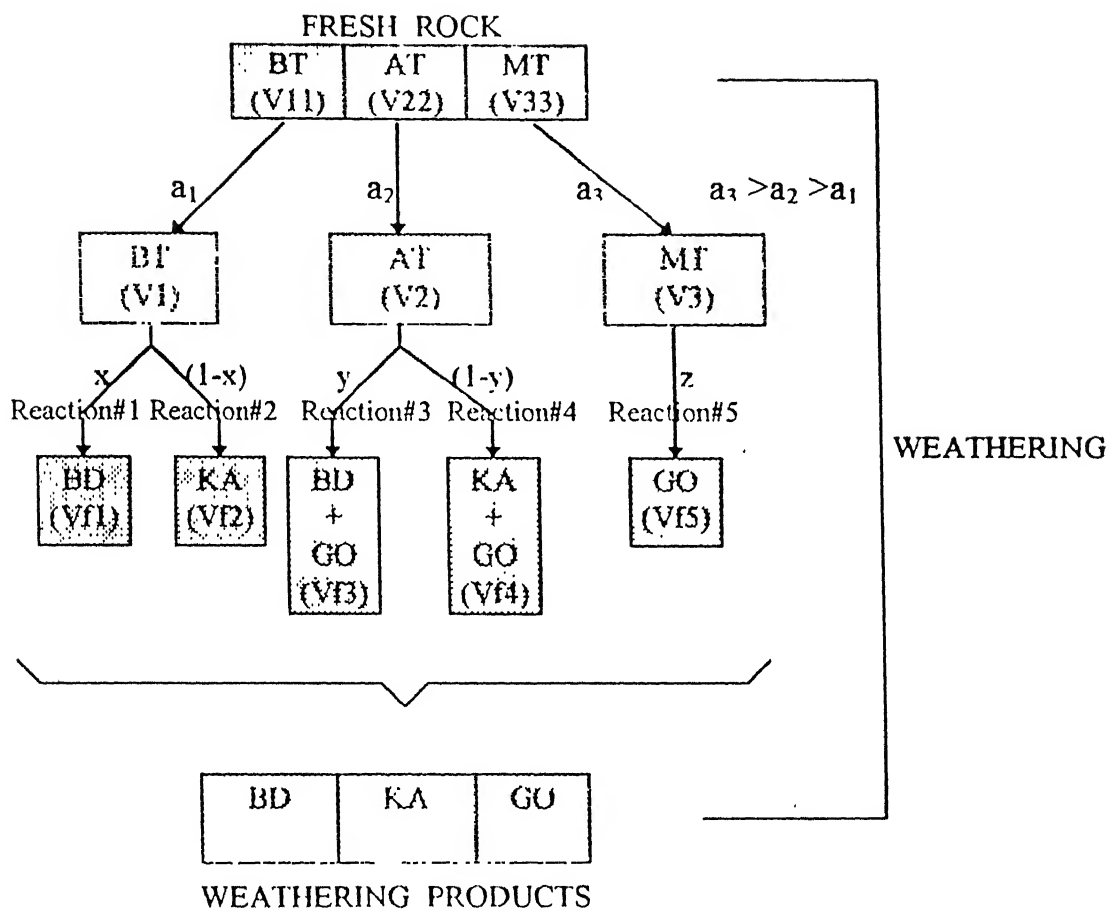


Fig. 4.7 Schematic Flow Diagram of Three-Mineral Model

CHAPTER-5

SUMMARY AND CONCLUSIONS

The area around Sagar University Campus in Madhya Pradesh contains excellent outcrops of Deccan basalt with typical spheroidal weathering features. This thesis work was taken up with the objective of outlining an overall mechanism of spheroidal weathering at microlevel on basaltic country rocks. The principal thrust of the present study was to identify appropriate weathering reactions relating primary and secondary minerals which cause volume expansion necessary for spheroidal weathering. The results of the present investigation involving fieldwork and laboratory analysis are summarized below.

5.1 MINERALOGY, TEXTURE AND GEOCHEMICAL CHANGE

- (i) The occurrence of four distinct basalt flows in the study area, as reported by earlier workers was confirmed by break in slopes and differences in their mode of weathering.
- (ii) Spheroidally weathered boulders of all the flows have a core of fresh rock surrounded by partly weathered innermost rindlets and loose friable outermost rindlets.
- (iii) Difference in size of the boulders in different flows is controlled by the joint spacing. In the study area, spheroidally weathered boulders of 7th flow are of relatively larger size as compared to other flows.
- (iv) Optical microscopy and X-ray diffraction analysis of the samples of fresh rock core established the presence of a Ca-plagioclase of bytownite composition, pyroxene of augite variety, magnetite and quartz.

(v) The innermost rindlets, immediately adjacent to the fresh rock core, retain nearly the same mineralogy and texture as the fresh rock core. But alteration of plagioclase to clay minerals along minute solution channels and grain boundaries was visible in thin section. In addition, partly hydrated halloysite identified in these rindlets can be considered as an alteration product. Reddish brown margins of these rindlets is obviously due to the oxidation of magnetite and mafic minerals. As shown earlier, weathering Reaction#3, Reaction#4, Reaction#5 are sensitive to the partial pressure of oxygen gas which is responsible for the oxidation of Fe^{-2} to Fe^{-3} .

(vi) The loose, friable outermost rindlets represent a more advanced stage of weathering. The slightly whitish colour of these rindlets are due to the presence of clay minerals. Characteristic tubular shape in SEM indicated that halloysite is one of the phases present. In other words, the innermost rindlets and outermost rindlets are similar in overall mineralogy but differ in their degree of weathering.

(vii) The final stage of weathering of Deccan basalt is the development of two types of residual soils - A black soil commonly observed in low grounds contains significant amount of beidellite (smectite). In contrast, a reddish-brown soil occurring at higher elevations is rich in halloysite (kaolinite) and iron-oxide (goethite?). Residual grains of quartz, plagioclase and augite in the soil indicated that all the primary minerals were not consumed during weathering.

(viii) X-ray mapping under EPMA across the section of a typical boulder showed that Fe and Ca are enriched towards the rim, whereas, Si, Al and Mg are enriched towards the core. SEM-EDX showed a pattern roughly similar with the EPMA results.

Enrichment of iron towards the rim is likely to be due to the precipitation of ferric oxide from leached ferrous iron. Higher proportion of Si, Al and Mg in the leached zone can be due to a residual concentration of aluminosilicate minerals like halloysite and beidellite.

(ix) Based on the mineralogy of reactants and products during weathering of Deccan basalt in the Sagar area, five representative reactions and the corresponding volume change can be represented as-

Reaction#1	4 Bytownite → 3 Beidellite	$\Delta V\% = +4.90$
Reaction#2	8 Bytownite → 7 Kaolinite	$\Delta V\% = -13.81$
Reaction#3	7 Augite → 6 Beidellite + 7 Goethite	$\Delta V\% = +6.91$
Reaction#4	2 Augite → 2 Kaolinite + 2 Goethite	$\Delta V\% = -9.35$
Reaction#5	2 Magnetite → 6 Goethite	$\Delta V\% = +40.09$

This indicates that volume expansion during weathering of rock forming minerals depends on the assemblage of secondary minerals.

An appropriate combination of the above five simultaneous reactions will result in a net positive ΔV , which is essential for spheroidal weathering. This relationship was quantified by a computer-aided three mineral model.

(x) The main conclusions from these model are

- Modal volume percentage of magnetite in fresh rock has a major influence in the net positive volume change.
- The maximum net positive volume change of 5.564% was obtained from 9th flow with initial modal composition of bytownite = 39.04%, augite = 45.87%, magnetite

= 4.74%; alteration fractions of $a_1 = 0.6$, $a_2 = 0.8$, $a_3 = 1.0$ and proportion of different reactions of $x = 0.50$, $y = 0.75$, $z = 1.00$.

- Calculated values of net $\Delta V\%$ for different flows can be different even with same combinations of a_1 , a_2 , a_3 and x , y , z . This is primarily because of a difference in initial modal volume percentage of primary minerals.

(xi) In addition to the above parameters the difference in mode of weathering in various flows can also be due to a variation in altitude, vegetation, slope and drainage.

5.2 OVERALL MECHANISM OF SPHEROIDAL WEATHERING

During cooling of basaltic lava flows tensional joints develop normal to the flow surface, which progressively split the rock into long prisms or columns termed as “columnar Joints”. Subsequently, infiltrating water moves along intersecting joint planes and attacks the enclosed rock mass from all sides gradually rounding of the edges and corners. Thus a spheroidal boulder is produced from the jointed basalt. The interior of the spheroidal mass, however, remains fresh. Leaching and migration of elements through solution channels give a pattern of diffusion rings around the fresh rock core. The concentric rindlets eventually crumble and fall off as a result of pressures set up within the rock during chemical weathering. The origin of this pressure is related to the fact that the weathering products occupy a greater volume than the parent material.

5.3 SUGGESTION FOR FURTHER WORK

- Confirmation of minerals like calcite, chlorophaeite, goethite/zeolite suspected in some samples, observed under optical microscope and SEM. Durge (1987) has identified a pale yellow and greyish green colour mineral pseudomorphous after pyroxene as

chlorophaeite. A similar property was noted in thin section of the innermost rindlets from 9th flow.

- More detailed analysis of variation in element concentration, particularly across solution channels adopting XRF method similar to the work of Augustithis and Ottemann (1966).
- Improvement of computer model incorporating modal composition of weathering product and exact mineral formulae in place of idealized composition.
- Comparison of the volume expansion calculated in the present computer model with real life data from construction materials and foundation rocks used in civil engineering projects.
- Extension of same technique to the weathering of the other flows of Deccan basalt in type areas.
- Estimation of weathering rate from rind thickness similar to the work of Colman (1986).
- Evaluation of the role of vegetation and microorganic processes in chemical weathering of basalt.

REFERENCES

- ALEXANDER, P.O., (1977). Geochemistry and Geochronology of Deccan Trap lava flows around Sagar, M.P., India; *Unpublished Ph.D thesis*, Dept. of Applied Geology, University of Sagar, M.P.
- AUGUSTITHIS, S.S. & OTTEMANN, J., (1966). On Diffusion Rings and Sphaeroidal Weathering; *Chem. Geol.*, vol.1, pp 201-209.
- AUGUSTITHIS, S.S. & VGENOPOULOS, A., (1983). On leaching and diffusion-rings in charnockites, basalt, trachytic tuffite, bauxite, alunite and andesite, in *"Leaching and Diffusion in Rocks and Their weathering Products"*; Theophrastus Publications S.A., Athens, Greece, pp 151-173.
- BILLINGS, M.P., (1990). *Structural Geology* (Third edition, 10th printing); Prentice Hall, Inc., New York.
- COLMAN, S.M., (1986). Levels of Time Information in Weathering Measurements, with Examples from Weathering Rinds on Volcanic Clasts in the Western United States, in *"Rates of Chemical weathering of Rocks and Minerals"*, S.M. Colman and D.P. Dethier Editors, Academic Press, Inc (London) Ltd., pp 379-392.
- DE GRAFF, J.M. & AYDIN, A., (1987). Surface morphology of columnar joints and its significance to mechanics and direction of joint growth; *Bull. Geol. Soc. Am.*, vol.99, pp 605-617.
- DEER, W.A., HOWIE, R.A. & ZUSSMAN, J., (1965). *Rock-forming Minerals*; vol.4. *Framework Silicates*, Longmans, Green and Co. Ltd., London.
- DURGE, M.V., (1987). Geology of Rocks of Patharia Hills, Saugor, M.P.; *Unpublished Ph.D thesis*, Dept. of Applied Geology, University of Saugor, M.P..
- FRITZ, S.J. & RAGLAND, P.C., (1980). Weathering rinds developed on plutonic igneous rocks in the North Carolina piedmont; *Am. Jour. Sci.*, vol.280, pp 546-559.
- FRITZ, S.J. & MOHR, D.W., (1984). Chemical alteration in the microweathering environment within a spheroidally - weathered anorthosite boulder; *Geochim. Cosmochim. Acta*, vol.48, pp 2527-2535.
- FRITZ, S.J., (1985). A comparative weathering study in the East Farrington adamellite and concord syenite; Reprint from *Southeastern Geology*, published at Duke University Durham, North Carolina, vol.25, No.3, pp 141-153.
- GARRELS, R.M. & CHRIST, C.L., (1965). *Solutions, Minerals and Equilibria*; Harper and Row, New York.

- GRIM, R.E.,(1968). *Clay Mineralogy* (Second edition); Mc Graw- Hill, New York.
- HESS, H.H. & POLDERVAART, A.,(1967). *Basalts, The Poldervaart treatise on rocks of basaltic composition*: Interscience, John Willey Sons, Inc., New York, vol.1 and vol.2.
- JUMIKIS, A.R.,(1979). *Rock Mechanics*; Trans Tech Publication, USA.
- KRAUSKOPF, K.B.,(1982). *Introduction to Geochemistry* (Second edition); Mc Graw-Hill International Student Edition, Singapore.
- KRISHNAN, M.S.,(1982). *Geology of India and Burma* (Sixth edition); CBS Publishers and Distributors, New Delhi.
- KRISHNASWAMY, V.S.,(1981). The Deccan Volcanic Episode, Related Tectonism and Geothermal Manifestations, in "Deccan Volcanism and Related Basalt Provinces in other parts of the World", K.V. Subbarao and R.N. Sukheshwala Editors, *Geol. Soc. India, Mem.* No.3, pp 1-7.
- LEET, L.D., & JUDSON, S.,(1965). *Physical Geology* (Third edition); Prentice Hall of India, New Delhi.
- LUNKAD, S.K.,(1975). Ground Water Quality and Soil Formation in Weathered Deccan Basalt of Malwa Plateau, M.P., India, *Unpublished M.Tech thesis*, Dept. of Civil Engg., IIT, Kanpur.
- LUNKAD, S.K., & RAYMAHASHAY, B.C.,(1978). Ground water quality in weathered Deccan Basalt of Malwa Plateau, India; *Quart. Jour. Engg. Geol.*, vol.11, pp 273-277.
- NAJAFI, S.J., COX, K.G. & SUKHESHWALA, R.N.,(1981). Geology and Geochemistry of the Basalt flows (Deccan traps) of the Mahad-Mahabaleshwar Section, India, in "Deccan Volcanism and Related Basalt Provinces in other parts of the world", K.V. Subbarao and R.N. Sukheshwala Editors, *Geol. Soc. India, Mem.* No.3, pp 300-315.
- RAYMAHASHAY, B.C.,(1996). *Geochemistry For Hydrologists*; Allied Publishers Ltd., New Delhi.
- SMALLEY, I.J.,(1966). Contraction crack networks in Basalt Flows, *Geol. Mag.*, vol.103, No.2, pp 111-114.
- SUBRAMANYAN, V.,(1981). Geomorphology of the Deccan Volcanic province, in "Deccan Volcanism and Related Basalt Provinces in other parts of the world",

- SUKHESWALA, R.N.,(1981). Deccan Basalt Volcanism, in “Deccan Volcanism and Related Basalt Provinces in other parts of the world”, K.V. Subbarao and R.N. Sukheshwala Editors. *Geol. Soc. India, Mem.* No.3, pp 8-18.
- TWISS, R.J. & MOORES, E.M.,(1992). *Structural Geology*; W.H. Freeman and Company; New York.
- WAHLSTROM, E.E.,(1955). *Petrographic Mineralogy*, John Willey and Sons, New York.
- WEST, W.D.,(1981). The duration of Deccan Trap Volcanicity, in “Deccan Volcanism and Related Basalt Provinces in other parts of the world”, K.V. Subbarao and R.N. Sukheshwala Editors, *Geol. Soc. India, Mem.* No.3, pp 277-278.
- WEST, W.D. & CHOUBEY, V.D.,(1964). The Geomorphology of the country around Sagar and Katangi, M.P. - An example of superimposed drainage, *Jour. Geol. Soc. Ind.*, Vol.5 pp 41-55.
- WILKINS, A., SUBBARAO, K.V., INGRAM, G. & WALSH, J.N.,(1994). Weathering Regimes within the Deccan Basalts, in “*Volcanism*” Radhakrishna volume, K.V. Subbarao Editor, Willey Eastern Limited, India, pp 217-231.

APPENDIX - I

Derivation of Surface Area for Different Prisms

Assume a spherical volume (V) of radius (r), and (001) face of the different prisms have equivalent radius (r).

For sphere,

$$V = \frac{4}{3} \pi r^3$$

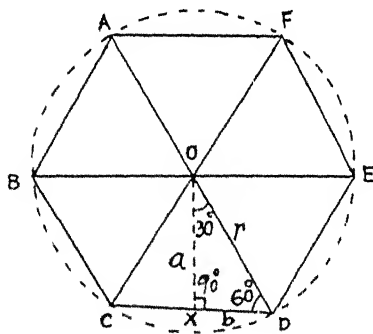
$$\frac{V}{r} = \frac{4}{3} \pi r^2$$

$$= 4.19 r^2$$

and, surface area, $S = 4 \pi r^2$

$$= 12.57 r^2$$

Hexagonal Prism



For $\triangle OXD$

$$\frac{a}{r} = \sin 60^\circ$$

$$\therefore a = r \frac{\sqrt{3}}{2}$$

$$\frac{b}{r} = \cos 60^\circ$$

$$\therefore b = \frac{r}{2}$$

Area of the top surface of the hexagonal prism

$$= 6 \times \frac{1}{2} \times 2b \times a$$

$$= 3 \times r \times r \times \frac{\sqrt{3}}{2}$$

$$= \frac{3\sqrt{3}}{2} r^2$$

If h_1 is the height of the hexagonal prism, then

$$\frac{3\sqrt{3}}{2} r^2 \times h_1 = V$$

$$\therefore h_1 = \frac{2r}{3\sqrt{3}} \times \frac{1}{r^2}$$

\therefore Total surface area of the hexagonal prism (SA_{Hexprism})

$$= 6(2b \times h_1) + 2\left(\frac{3\sqrt{3}}{2} r^2\right)$$

$$= 6 \times 2 \times \frac{r}{2} \times \frac{2v}{3\sqrt{3}} \times \frac{1}{r^2} + 2 \times \frac{3\sqrt{3}}{2} r^2$$

$$= \frac{4}{\sqrt{3}} \left(\frac{V}{r} \right) + 3\sqrt{3} r^2$$

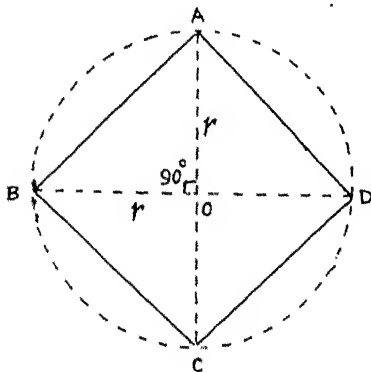
$$= 2.31 \left(\frac{V}{r} \right) + 5.196 r^2$$

$$= 2.31 \times 4.19 r^2 + 5.196 r^2$$

$$= 9.676 r^2 + 5.196 r^2$$

$$\therefore \boxed{SA_{\text{Hexprism}} = 14.87 r^2 \text{ sq. unit}}$$

Square Prism



$$a = \sqrt{2} r$$

Area of the top surface of the square prism

$$= (\sqrt{2} r)^2$$

$$= 2 r^2$$

If h_2 is the height of the square prism, then

$$2 r^2 \times h_2 = v$$

$$\Rightarrow h_2 = \frac{V}{2r^2}$$

Total surface area of the square prism (SA_{prism})

$$= 4 \times \sqrt{2} r \times h_2 + 2 \times 2r^2$$

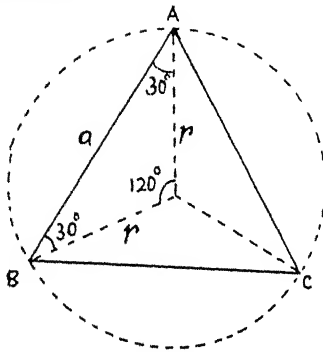
$$= 2\sqrt{2} \frac{V}{r} + 4r^2$$

$$= 2.83 \times 4.19 r^2 + 4r^2$$

$$= 15.86 r^2$$

$$\therefore SA_{\text{prism}} = 15.86 r^2 \text{ sq. unit}$$

Triangular Prism



In ΔAOB

$$\frac{r}{\sin 30^\circ} = \frac{r}{\sin 30^\circ} = \frac{a}{\sin 120^\circ}$$

$$\therefore a = \frac{r \sin 120^\circ}{\sin 30^\circ} = \sqrt{3} r$$

$$\text{Half perimeter (S)} = \frac{3\sqrt{3}}{2} r$$

Area of the top surface of the triangular prism

$$= \sqrt{S(S-a)(S-r)(S-r)} r$$

$$= \sqrt{\frac{3r\sqrt{3}}{2} \left(\frac{3r\sqrt{3}}{2} - r\sqrt{3} \right) \left(\frac{3r\sqrt{3}}{2} - r\sqrt{3} \right) \left(\frac{3r\sqrt{3}}{2} - r\sqrt{3} \right)}$$

$$= \frac{3r^2}{4} \sqrt{3}$$

If h_3 is the height of the triangular prism, then

$$\frac{3r^2}{4} \sqrt{3} \times h_3 = V$$

$$\Rightarrow h_3 = \frac{4V}{3r^2\sqrt{3}}$$

Total surface area of the triangular prism (SA_{Triprism})

$$= 3 \times h_3 \times a + \frac{2 \times 3r^2\sqrt{3}}{4}$$

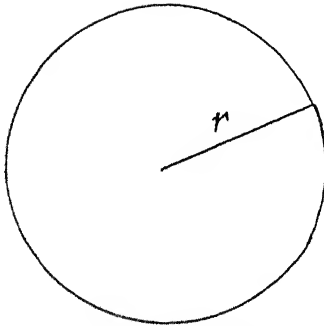
$$= 4\left(\frac{V}{r}\right) + \frac{3r^2\sqrt{3}}{2}$$

$$= 16.76r^2 + 2.59r^2$$

$$= 19.35r^2$$

$$\therefore \boxed{SA_{\text{Triprism}} = 19.35r^2 \text{ sq. unit}}$$

Cylinder



If h_4 is the height of the cylinder

$$\pi r^2 \times h_4 = V$$

$$\Rightarrow h_4 = \frac{V}{\pi r^2}$$

Total surface area of the cylinder ($SA_{\text{cyl.}}$)

$$= 2\pi r h_4 + 2\pi r^2$$

$$= 2\frac{V}{r} + 2\pi r^2$$

$$= 2 \times 4.19r^2 + 6.28r^2$$

$$= 23.04r^2$$

$$\therefore \boxed{SA_{\text{cyl.}} = 23.04r^2}$$

APPENDIX - II

4 BYTOWNITE \Rightarrow 3 BEIDELLITE
 8 BYTOWNITE \Rightarrow 7 KAOLINITE
 7 AUGITE \Rightarrow 6 BEIDELLITE + 7 GOETHITE
 2 AUGITE \Rightarrow 2 KAOLINITE + 2 GOETHITE
 2 MAGNETITE \Rightarrow 6 GOETHITE

Reaction#1
 Reaction#2
 Reaction#3
 Reaction#4
 Reaction#5

<u>Minerals</u>	<u>Composition</u>	<u>Mol.wt.</u>	<u>Sp.gr.</u>
BYTOWNITE (BT):	$\text{Na}_{0.25}\text{Ca}_{0.75}\text{Al}_{1.75}\text{Si}_{2.25}\text{O}_8$	274.22	2.72
BEIDELLITE (BD):	$\text{Ca}_{0.17}\text{Al}_{2.33}\text{Si}_{3.67}\text{O}_{10}(\text{OH})_2$	366.64	2.60
KAOLINITE (KA):	$\text{Al}_2\text{Si}_2\text{O}_5(\text{OH})_4$	258.17	2.60
AUGITE (AT):	$\text{CaMgFeAl}_2\text{Si}_3\text{O}_{12}$	450.47	3.40
MAGNETITE(MT):	Fe_3O_4	231.55	5.20
GOETHITE (GO):	FeO.OH	089.00	4.28

$$\text{Molar Volume} = \frac{\text{Molecular Weight}}{\text{Specific Gravity}}$$

V11 = modal vol. (%) of BYTOWNITE in fresh rock

V22 = modal vol. (%) of AUGITE in fresh rock

V33 = modal vol. (%) of MAGNETITE in fresh rock

v1 = vol. (%) of BYTOWNITE altered

v2 = vol. (%) of AUGITE altered

v3 = vol. (%) of MAGNETITE altered

F1 = vol. (%) of BYTOWNITE unaltered

F2 = vol. (%) of AUGITE unaltered

F3 = vol. (%) of MAGNETITE unaltered

VBT1 = molar vol. change in Reaction#1

VBT2 = molar vol. change in Reaction#2

VAT1 = molar vol. change in Reaction#3

VAT2 = molar vol. change in Reaction#4

VMT = molar vol. change in Reaction#5

a1 = alteration factor for BYTOWNITE

a2 = alteration factor for AUGITE

a3 = alteration factor for MAGNETITE

x = proportion of reaction between Reaction#1 and Reaction#2

y = proportion of reaction between Reaction#3 and Reaction#4

z = proportion of reaction in Reaction#5

vi1 = reactant vol. in Reaction#1

vi2 = reactant vol. in Reaction#2

vi3 = reactant vol. in Reaction#3
 vi4 = reactant vol. in Reaction#4
 vi5 = reactant vol. in Reaction#5
 vc1 = vol. change in Reaction#1
 vc2 = vol. change in Reaction#2
 vc3 = vol. change in Reaction#3
 vc4 = vol. change in Reaction#4
 vc5 = vol. change in Reaction#5
 vf1 = product vol. in Reaction#1
 vf2 = product vol. in Reaction#2
 vf3 = product vol. in Reaction#3
 vf4 = product vol. in Reaction#4
 vf5 = product vol. in Reaction#5
 VC = net vol. change in percentage

COMPUTER PROGRAM

```

#include <stdio.h>
#define VBT1 0.049
#define VBT2 -0.138
#define VAT1 0.069
#define VAT2 -0.093
#define VMT 0.401

main ( )
{
    float x, y, z;
    float V11, V22, V33, a1, a2, a3;
    float v1, v2, v3;
    float vi1, vi2, vi3, vi4, vi5;
    float vc1, vc2, vc3, vc4, vc5;
    float vf1, vf2, vf3, vf4, vf5;
    float F1, F2, F3, VC;
    printf ( " ENTER THE MODAL PERCENTAGE OF BYTOWNITE AUGITE
    MAGNETITE \n " );
    scanf ( " %f%f%f", &V11, &V22, &V33 );
    printf ( " %5.2f \t %5.2f \t %5.2f \n ", V11, V22, V33 );
    printf ( " ENTER THE VALUE OF a1 a2 a3 \n " );
  
```

[illegible]

TABLE 4.9 COMPUTER OUTPUT

6th FLOW

Modal volume percentage of Bvtownite=41.61, Augite=48.48, Magnetite=9.90

0.2	0.4	0.6	0.50	0.50	1.00	1.769
			0.25	0.50	1.00	1.380
			0.75	0.50	1.00	2.158
			0.50	0.75	1.00	2.554
			0.25	0.25	1.00	0.594
			0.75	0.25	1.00	1.373
			0.25	0.75	1.00	2.165
0.4	0.6	0.8	0.50	0.50	1.00	2.076
			0.25	0.50	1.00	1.298
			0.75	0.50	1.00	2.854
			0.50	0.75	1.00	3.254
			0.25	0.25	1.00	0.120
			0.75	0.25	1.00	1.676
			0.25	0.75	1.00	2.476
0.6	0.8	1.0	0.50	0.50	1.00	2.384
			0.25	0.50	1.00	1.216
			0.75	0.50	1.00	3.551
			0.50	0.75	1.00	3.954
			0.25	0.25	1.00	-0.354
			0.75	0.25	1.00	1.980
			0.25	0.75	1.00	2.787

7th FLOW

Modal volume percentage of Bvtownite=47.01, Augite=46.18, Magnetite=6.79

0.2	0.4	0.6	0.50	0.50	1.00	0.974
			0.25	0.50	1.00	0.534
			0.75	0.50	1.00	1.413
			0.50	0.75	1.00	1.722
			0.25	0.25	1.00	-0.214
			0.75	0.25	1.00	0.665
			0.25	0.75	1.00	1.282
0.4	0.6	0.8	0.50	0.50	1.00	0.989
			0.25	0.50	1.00	0.110
			0.75	0.50	1.00	1.868
			0.50	0.75	1.00	2.111
			0.25	0.25	1.00	-1.012
			0.75	0.25	1.00	0.746
			0.25	0.75	1.00	1.232
0.6	0.8	1.0	0.50	0.50	1.00	1.004
			0.25	0.50	1.00	-0.314
			0.75	0.50	1.00	2.328
			0.50	0.75	1.00	2.501
			0.25	0.25	1.00	-1.811
			0.75	0.25	1.00	0.827
			0.25	0.75	1.00	1.182

8TH FLOW

Modal volume percentage of Bytownite=41.38, Augite=49.48, Magnetite=9.12

0.2	0.4	0.6	0.50	1.586
			0.25	1.182
			0.75	1.955
			0.50	2.370
			0.25	0.380
			0.75	1.154
			0.25	1.983
0.4	0.6	0.8	0.50	1.813
			0.25	1.039
			0.75	2.587
			0.50	3.015
			0.25	-0.163
			0.75	1.384
			0.25	2.241
0.6	0.8	1.0	0.50	2.057
			0.25	0.897
			0.75	3.218
			0.50	3.660
			0.25	-0.707
			0.75	1.615
			0.25	2.500

9TH FLOW

Modal volume percentage of Bytownite=39.04, Augite=45.87, Magnetite=14.74

0.2	0.4	0.6	0.50	2.629
			0.25	2.264
			0.75	2.994
			0.50	3.372
			0.25	1.521
			0.75	2.251
			0.25	3.007
0.4	0.6	0.8	0.50	0.353
			0.25	2.623
			0.75	4.083
			0.50	4.468
			0.25	1.509
			0.75	2.969
			0.25	3.738
0.6	0.8	1.0	0.50	4.078
			0.25	2.983
			0.75	5.173
			0.50	5.564
			0.25	1.497
			0.75	3.687
			0.25	4.469